Practical Implementation of pCT Algorithms

BLAKE E. SCHULTZE

BAYLOR UNIVERSITY

Presentation Topics

1) Hull-detection: Development for object boundary detection
2) MLP Formalism: Development of a computationally efficient implementation
3) TVS: Applying recent methodological advances in theory to pCT

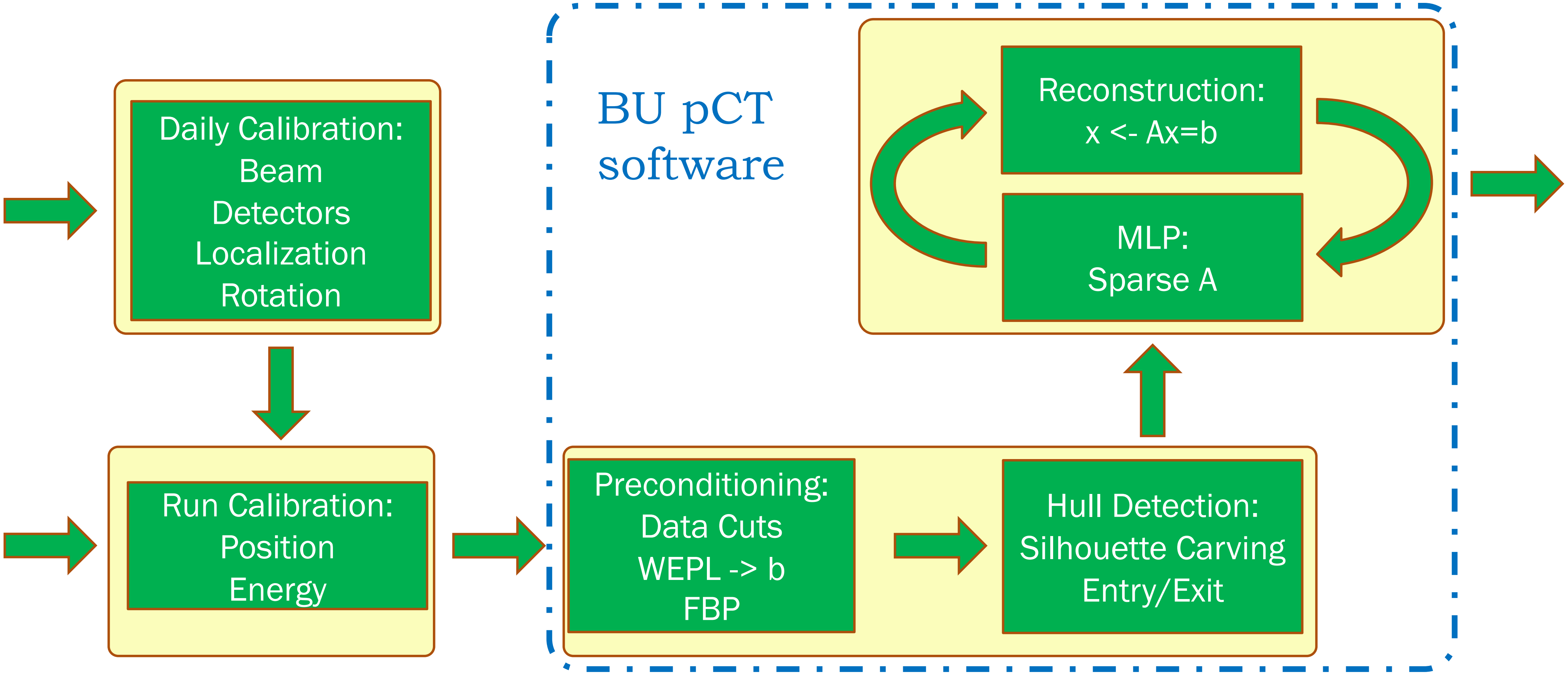

pCT Data Flow

- BU pCT software performs preconditioning and image reconstruction steps

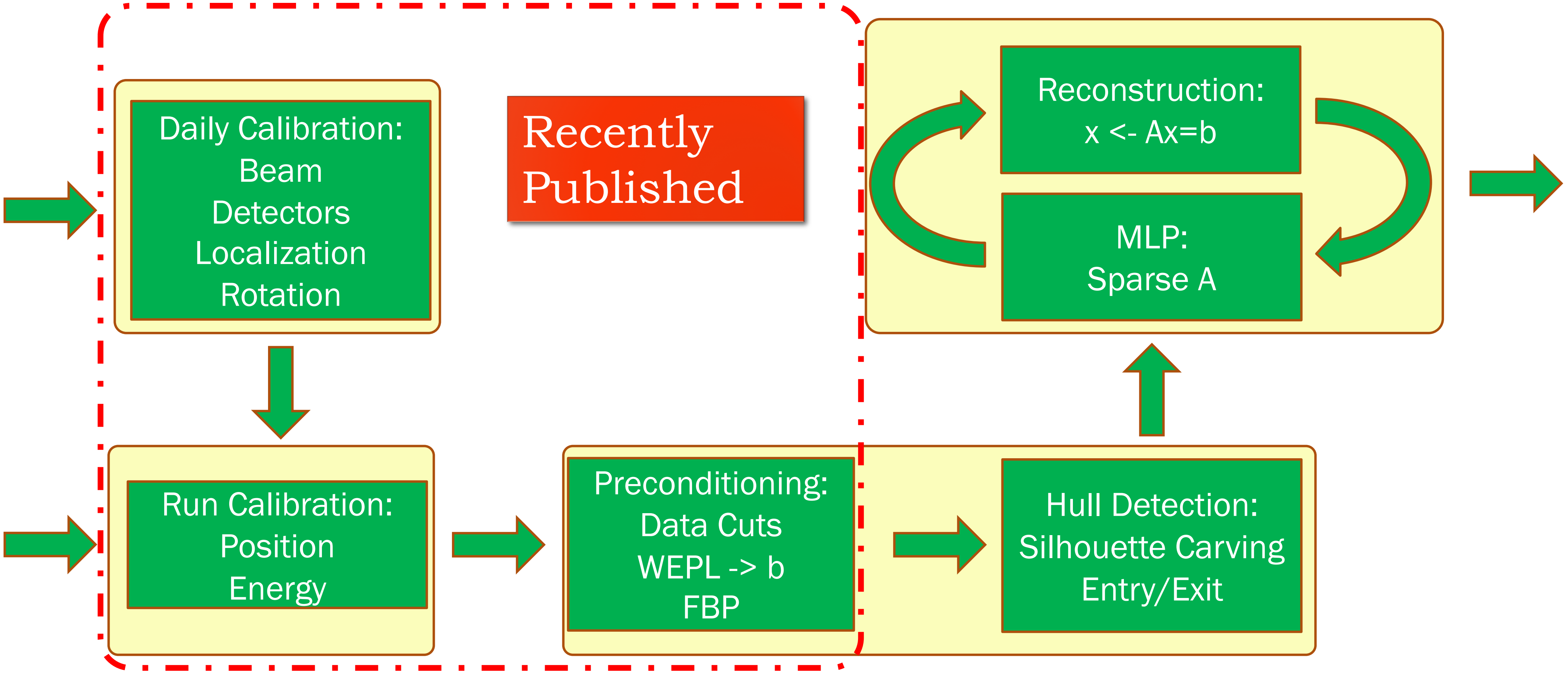

Data Acquisition, Preprocessing, & Preconditioning

Detailed description of these steps published in *IEEE Access* (2021)

“Particle-tracking proton computed tomography—data acquisition, preprocessing, and preconditioning”

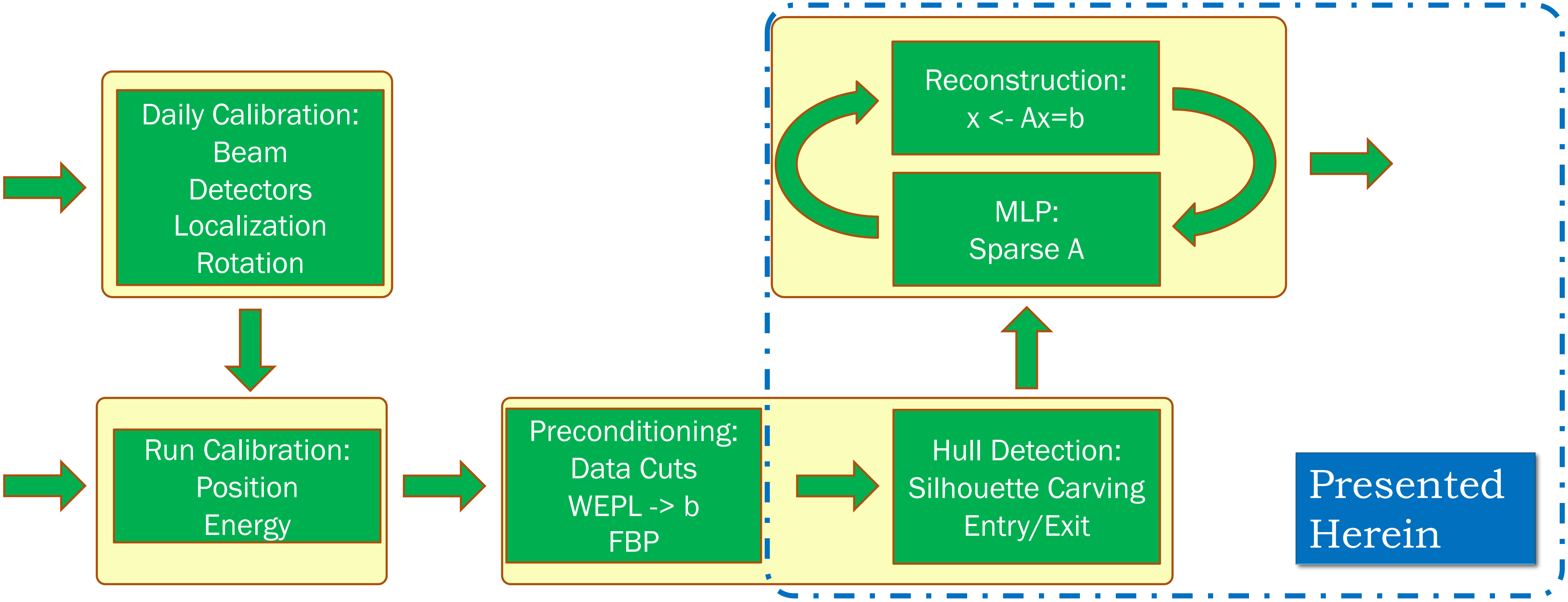

Data Acquisition & Preprocessing

Detailed description of these steps published in *IEEE Access* (2021)

“Particle-tracking proton computed tomography—data acquisition, preprocessing, and preconditioning”

Hull-Detection

Object
Boundary
Detection

Object boundary detection is…

- used to determine if/where a proton entered/exited the object
- used to restrict reconstruction to protons traversing object
- used to restrict the reconstruction image space solely to those voxels within the object

- Published: *Contemporary Mathematics, Vol. 36* (2015)

"Performance of hull-detection algorithms for proton computed tomography reconstruction"

BAYLOR UNIVERSITY 1845

Object Boundary Detection: Advantages of Hull-Detection?

- can begin during pCT scans, i.e. online mode
- parallelizable & relatively fast (~5 seconds)
- hull can define mask for spatially filtering x_0 ⇒ restricts image space to relevant voxels
- more reliable object entry & exit coordinates
  - key to proton path estimation
- can identify & exclude protons missing object

Silhouette Carving (SC) Method

- Fundamental Concepts

- Protons missing object…
  - experience negligible scattering & energy loss in air
  - travel along approximate straight line paths (SLP)
  - identifiable by WEPL and/or angular deviation
- Voxels along SLPs can be identified & excluded from hull
- Voxels not excluded after repeating for many protons defines object hull

Silhouette Carving (SC) Method

- Implementation Details

- Hull initialized to entire image space
- Protons missing object identified by

$$\text{WEPL} < -1\ \text{mm}$$

- Voxel walk algorithm (3D-DDA) developed to identify voxels along each proton path
- Based on 2D ray marching method: digital difference analyzer (DDA)
- 3D-DDA is efficient/accurate & numerically stable

Voxel Carving Process

1) Starting from hull encompassing image space
2) Identify voxels intersected by 1st proton missing object

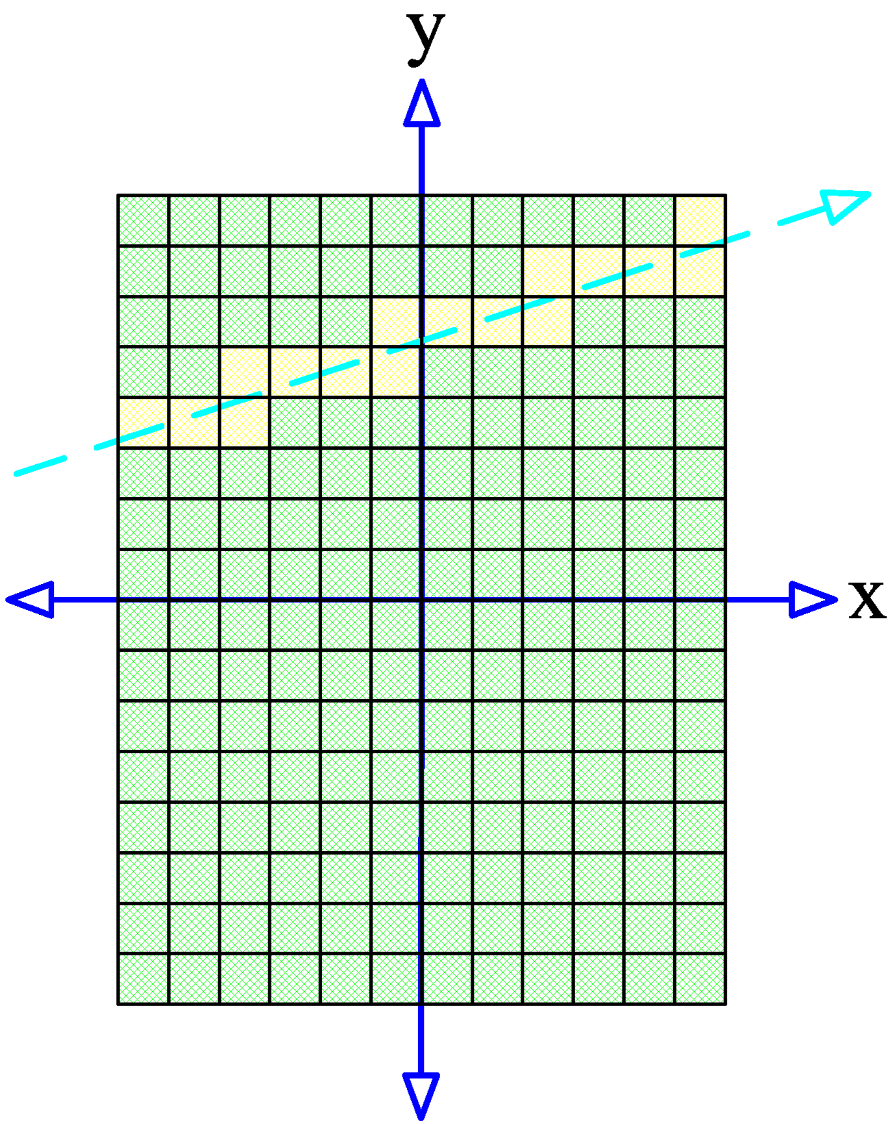

Voxel Carving Process

3) Carve (remove) voxels intersected by 1st proton

4) Identify voxels intersected by 2nd proton missing object

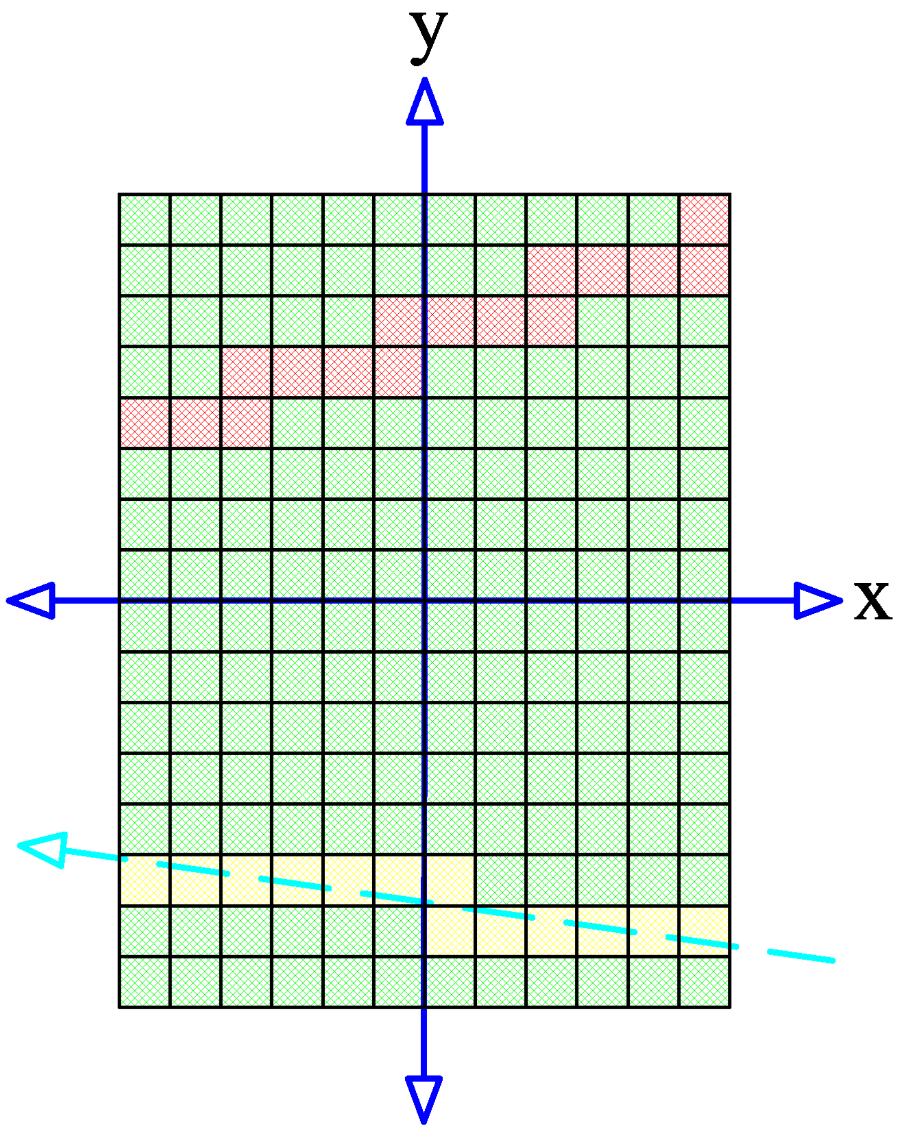

Voxel Carving Process

6) Carve (remove) voxels intersected by 2nd proton

7) Identify voxels intersected by 3rd proton missing object

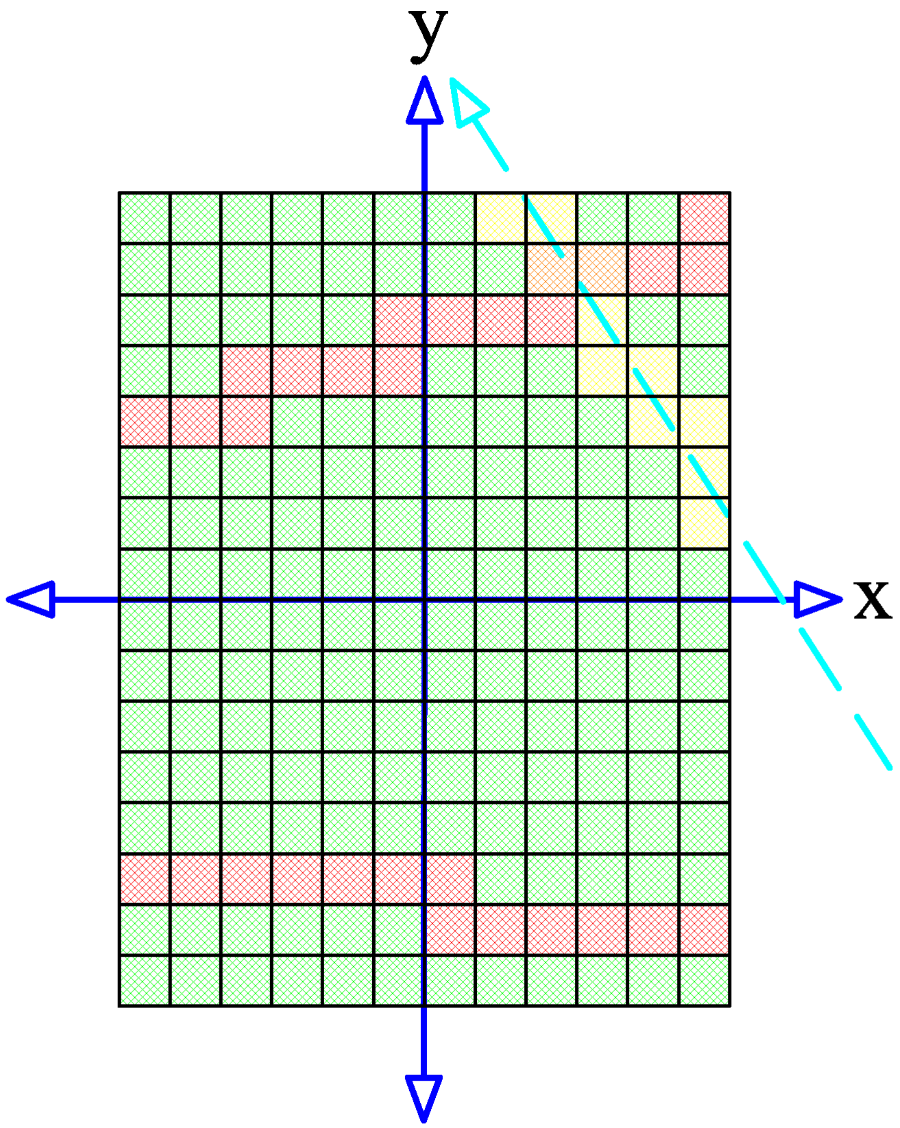

Voxel Carving Process

7) Repeat preceding steps for all protons missing object
8) Remaining voxels define object hull

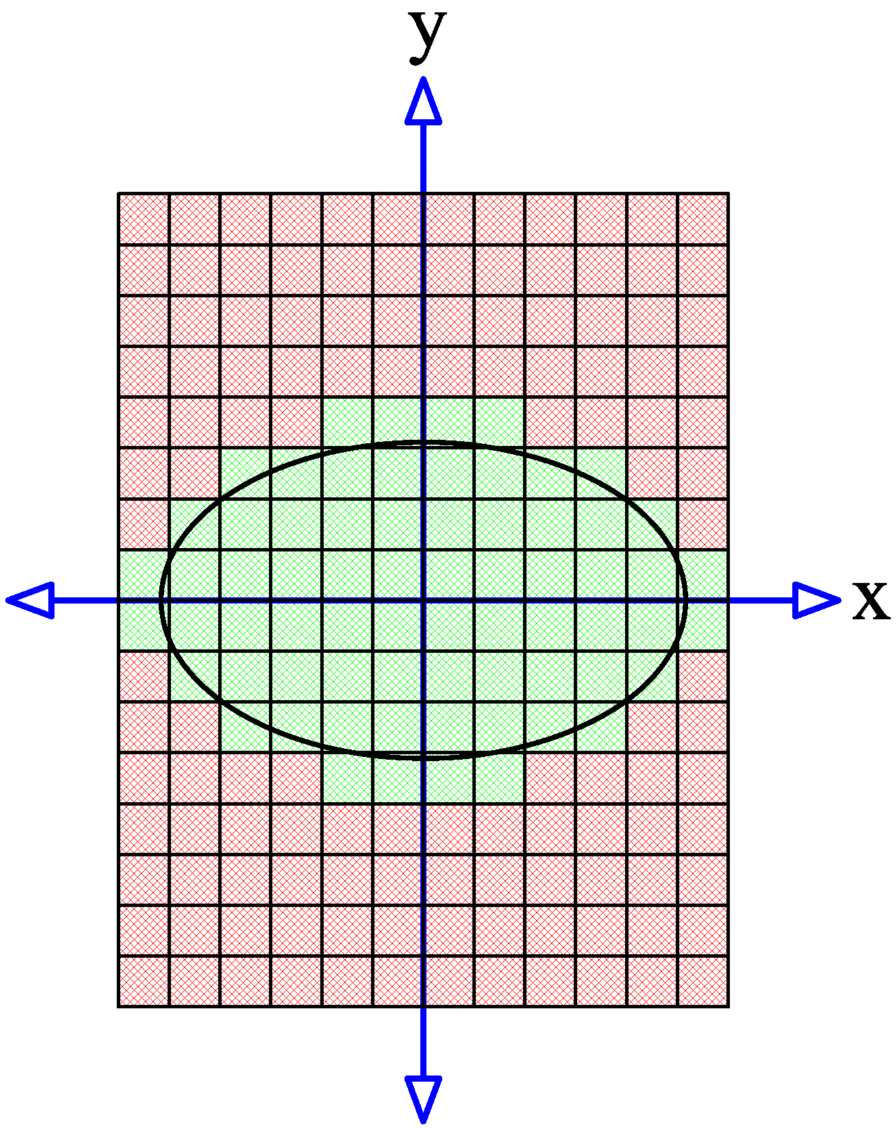

Initial Simulated pCT Data Investigations

Noiseless | Noisy (Gaussian)

Silhouette Carving

Thresholded Filtered Backprojection

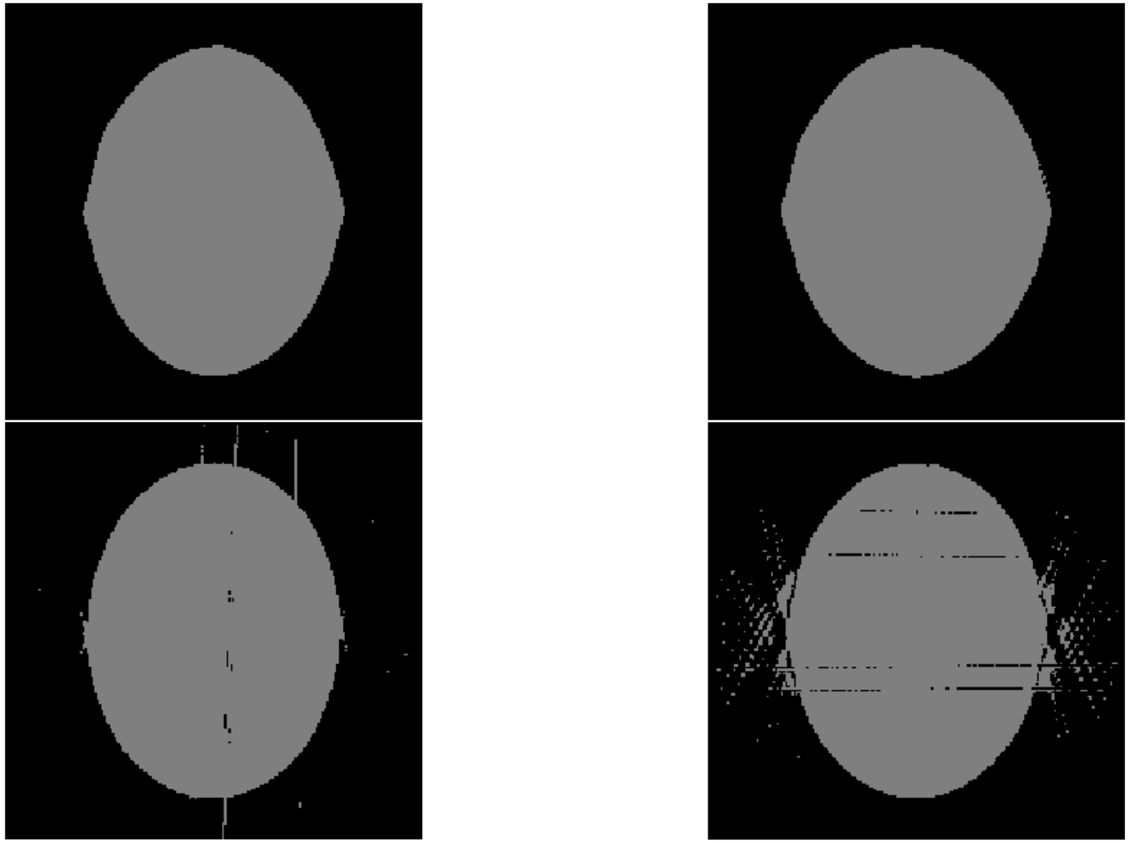

Experimental (real) pCT Data Investigations

	Rat Head	Pediatric Head Phantom
Silhouette Carving	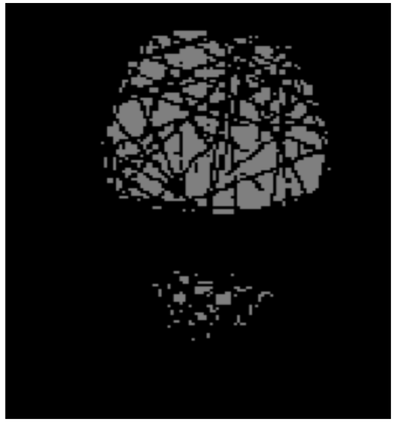	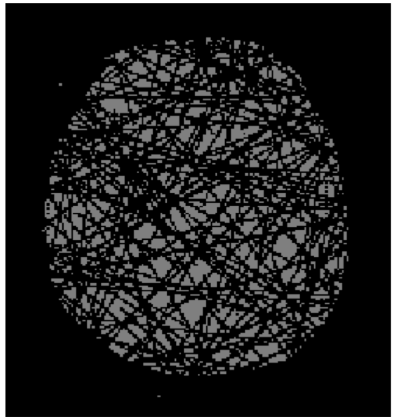
Thresholded Filtered Backprojection	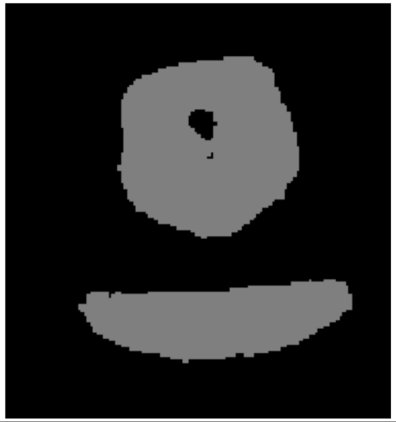	

Rectifying Observed SC Deficiency

1) Silhouette Carving (SC) was adapted to use binned data after removing unsuitable proton histories

2) Modified Silhouette Carving (MSC) algorithm developed
   a) Counts # of times voxel identified outside object
   b) Uses counts to identify voxels to exclude from hull

3) Space Modeling (SM) algorithm developed
   a) Uses protons entering object to construct hull
   b) Counts # of times voxel identified within object
   c) Uses counts to identify voxels to include in hull

Experimental (real) pCT Data Investigations

SC | MSC | Thresholded FBP

Pediatric Head Phantom

Rat Head

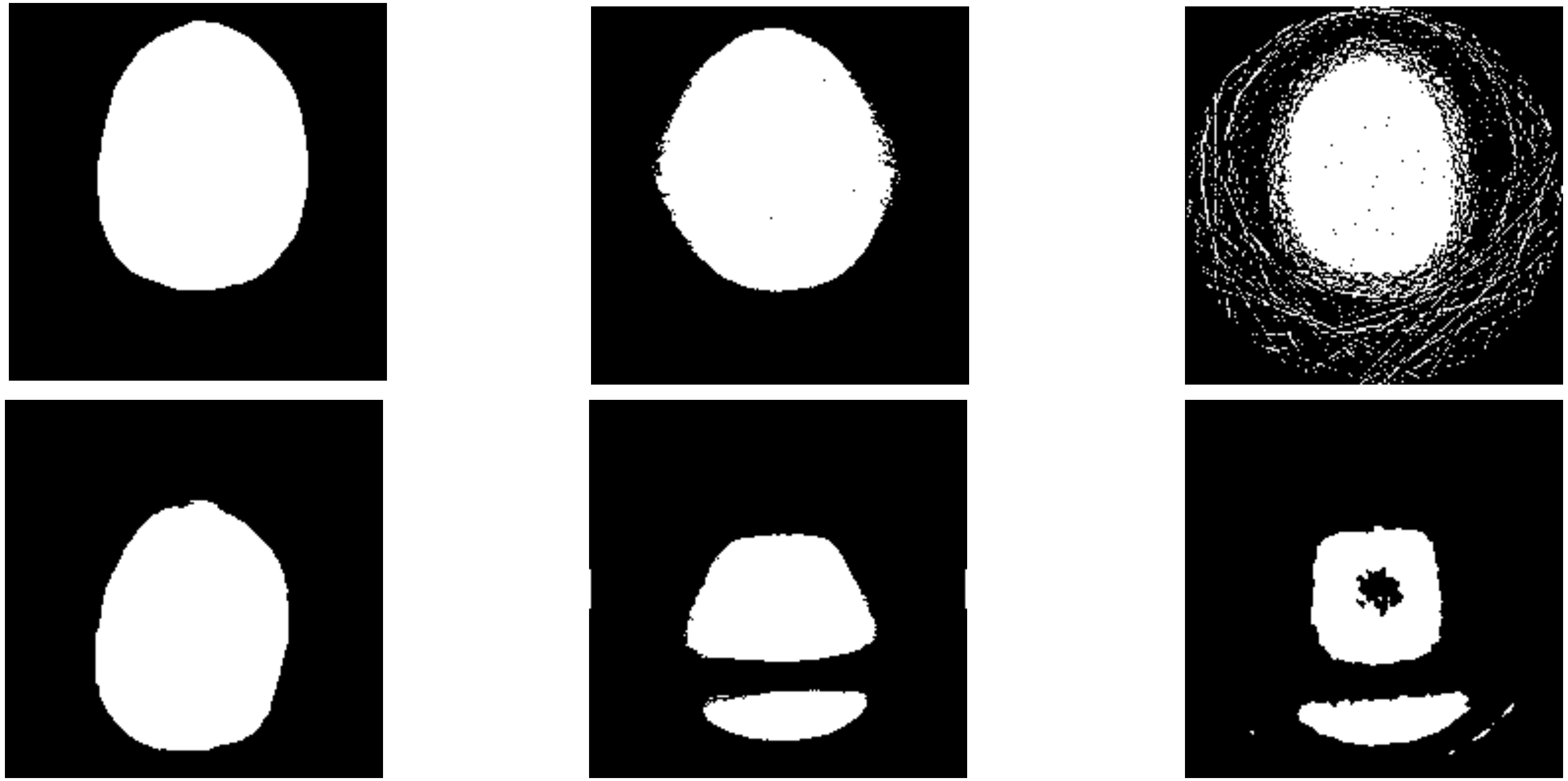

Hull-Detection Viability Conclusions

- SC generated most accurate hulls, but requires unsuitable data removal & proton data binning
- MSC slightly less accurate than SC, but supports online-mode & doesn't require unsuitable data removal
- SC & MSC are viable hull-detection algorithms w/ potential for improvements

Hull-Detection: Unpublished Updates

- MSC is currently the preferred hull-detection algorithm as a result of the following developments:
  - much larger (~350 million protons) data sets
  - flagged protons (WEPL = −100 mm) removed & no longer interfere
  - scans w/ continuous range of beamline angles
- MSC performs well under these conditions & has preferred characteristics, though it can still be improved

MLP Formalism

Efficient Computation & Data Storage

Most-Likely Path (MLP) is…

- used to approximate proton paths through object
- used to define hyperplanes (i.e. rows of system matrix $\boldsymbol{A} \in \mathbb{R}^{m \times n}$)
- the most computationally expensive step of pCT

- Publication in Preparation: *IEEE Access*

“Particle-tracking proton computed tomography—image reconstruction”

Problem Size

$m \sim 10^9$ Proton Histories

$n \sim 10^7$ Image Space Voxels

~ 400 Voxels/MLP

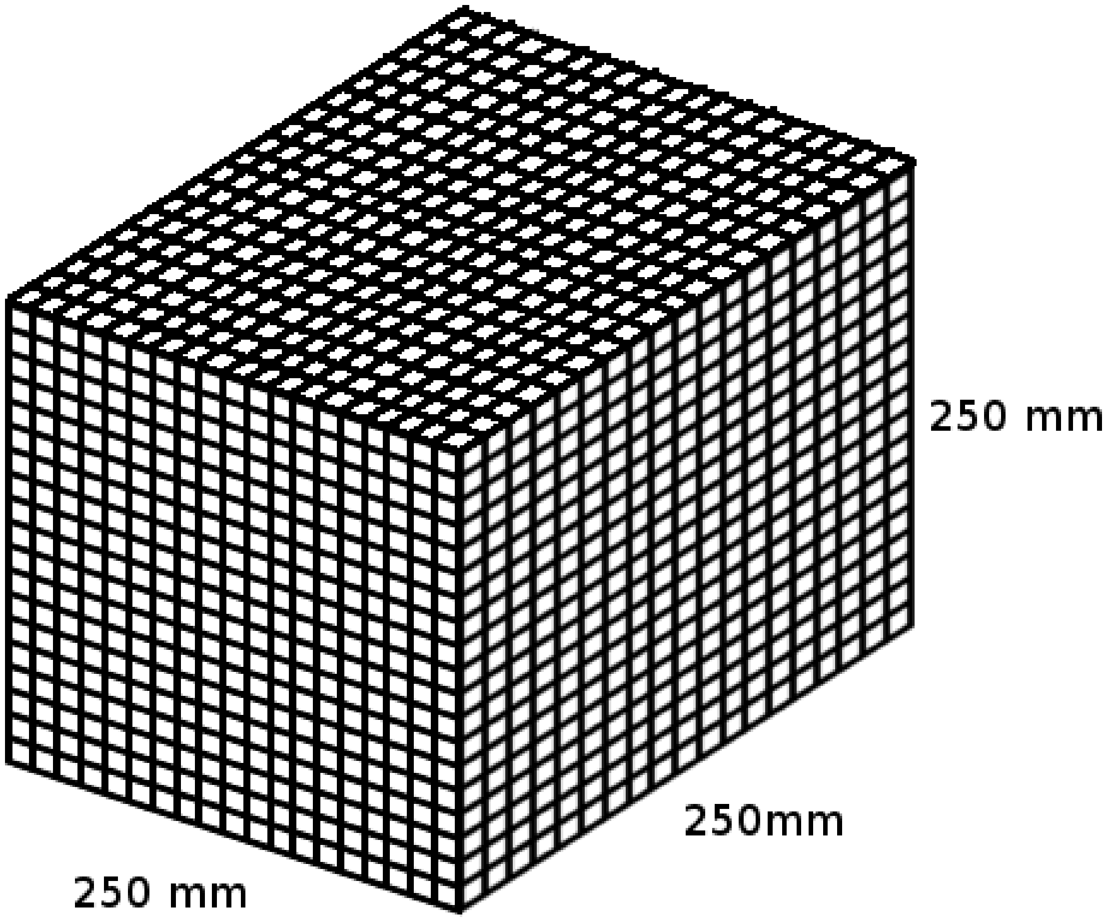

$$A \in \mathbb{R}^{m \times n} \Rightarrow size(A) = m \cdot n = \sim 10^9 \cdot \sim 10^7 = \sim 10^{16}$$

$$\Rightarrow sparsity(A) = \sim 400 \cdot \frac{10^9}{10^{16}} = \sim 4 \cdot 10^{-5} = 0.040\%$$

MLP

- Highly sparse ***A*** matrix
- CSR is common sparse matrix format
- Much more efficient than dense matrix storage

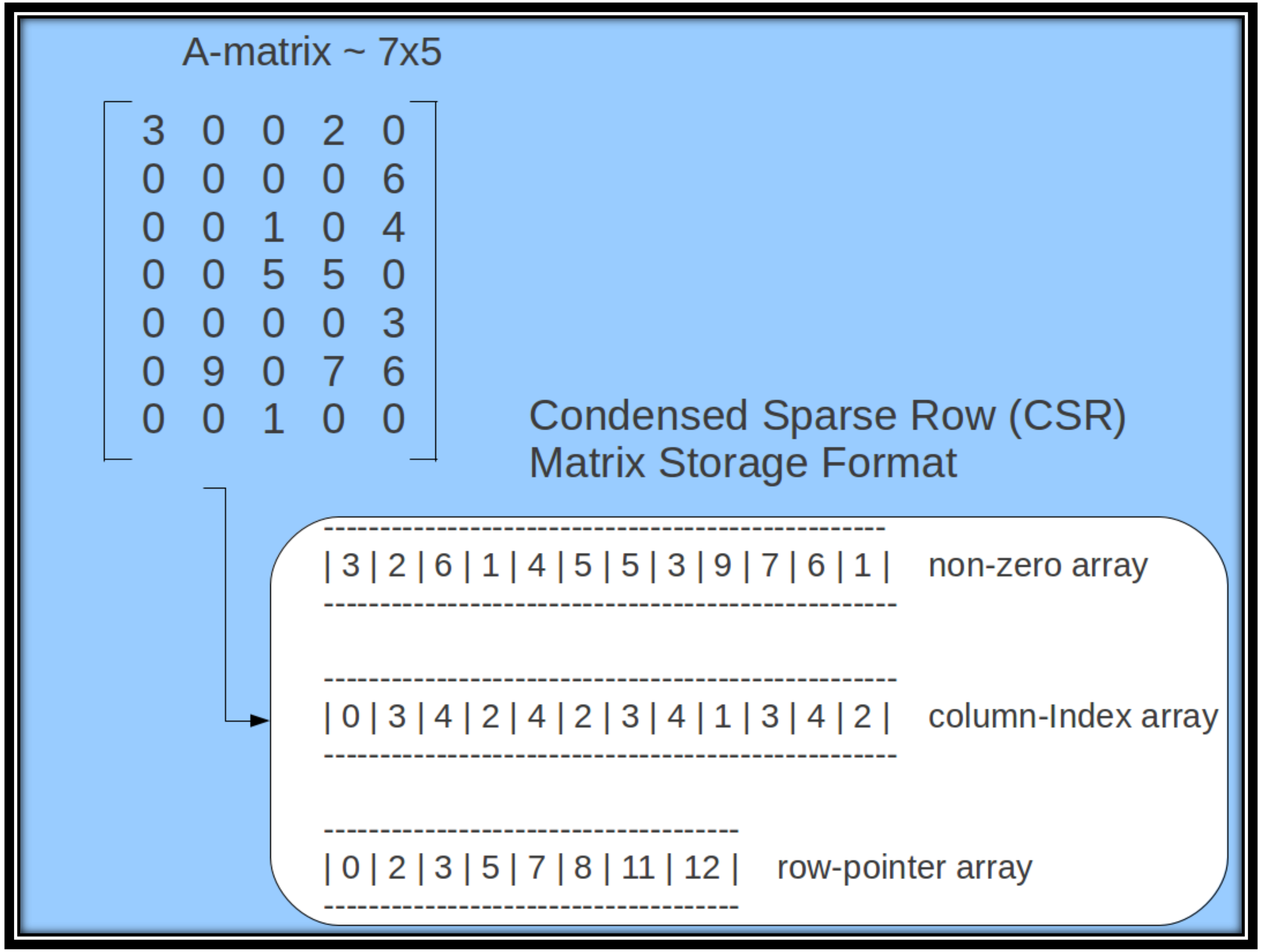

MLP

- FS only processes individual rows of ***A*** matrix
- Each row has single value path length
- More efficient to store only the indices of each voxel intersected by MLP

Intersected Voxel Identification

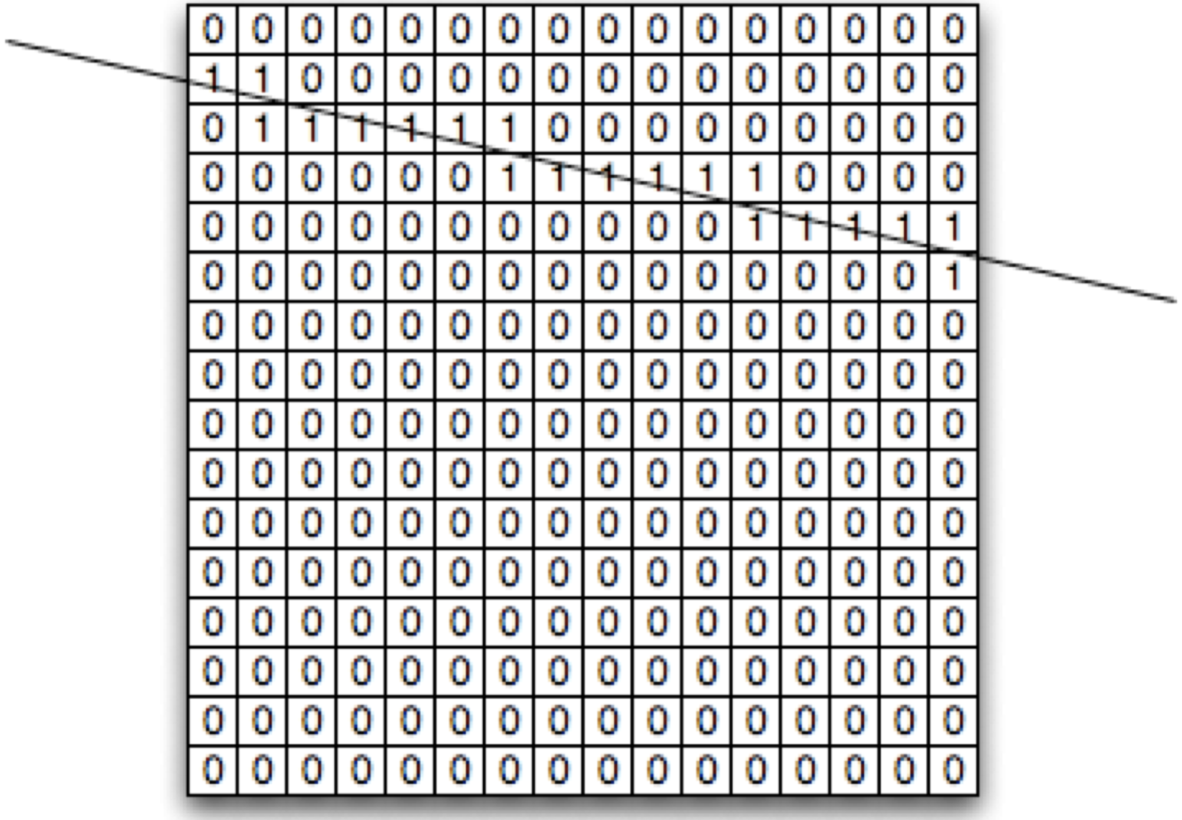

Current MLP Storage Scheme

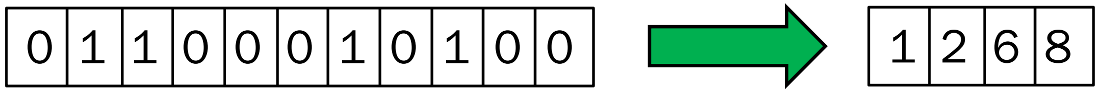

MLP — Conceptual Path & Proton Coordinate System

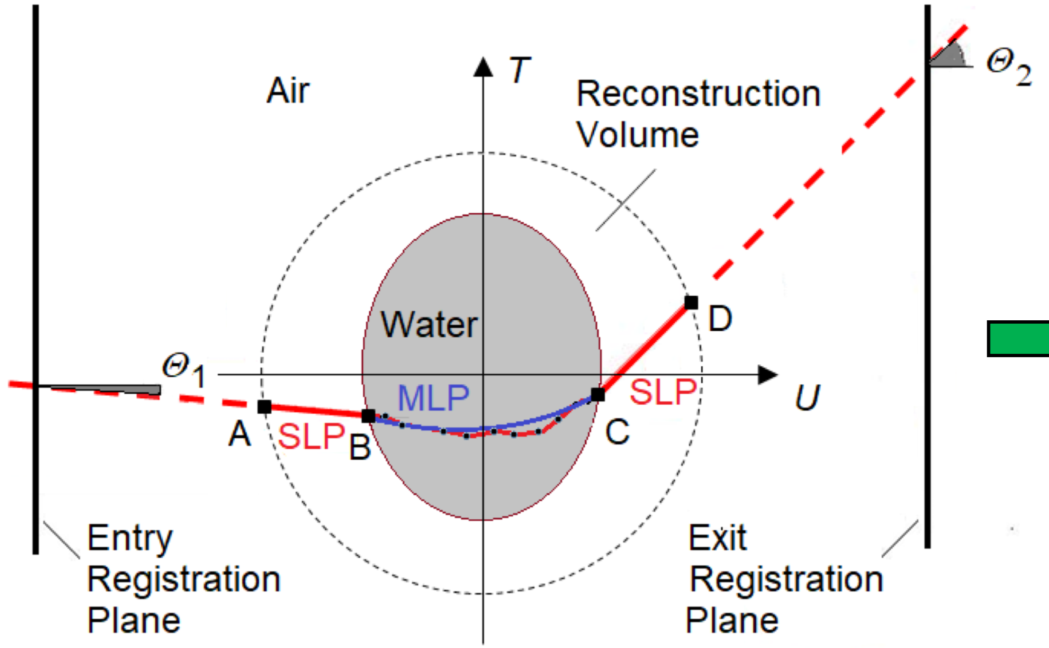

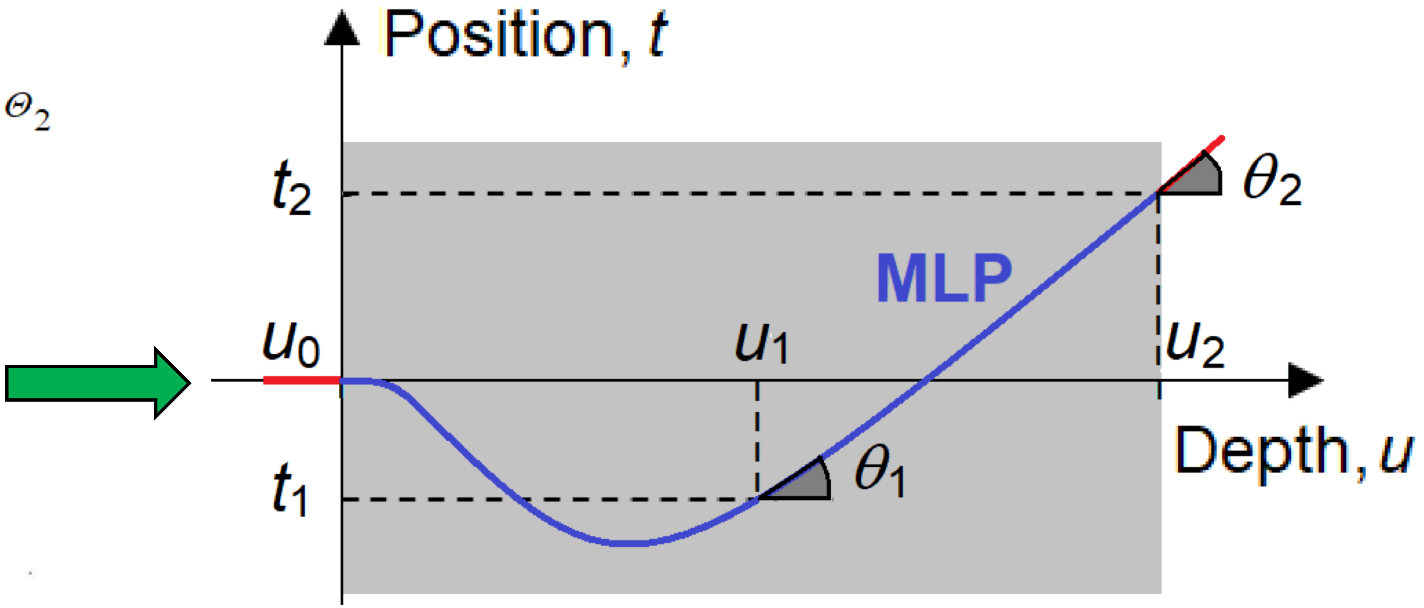

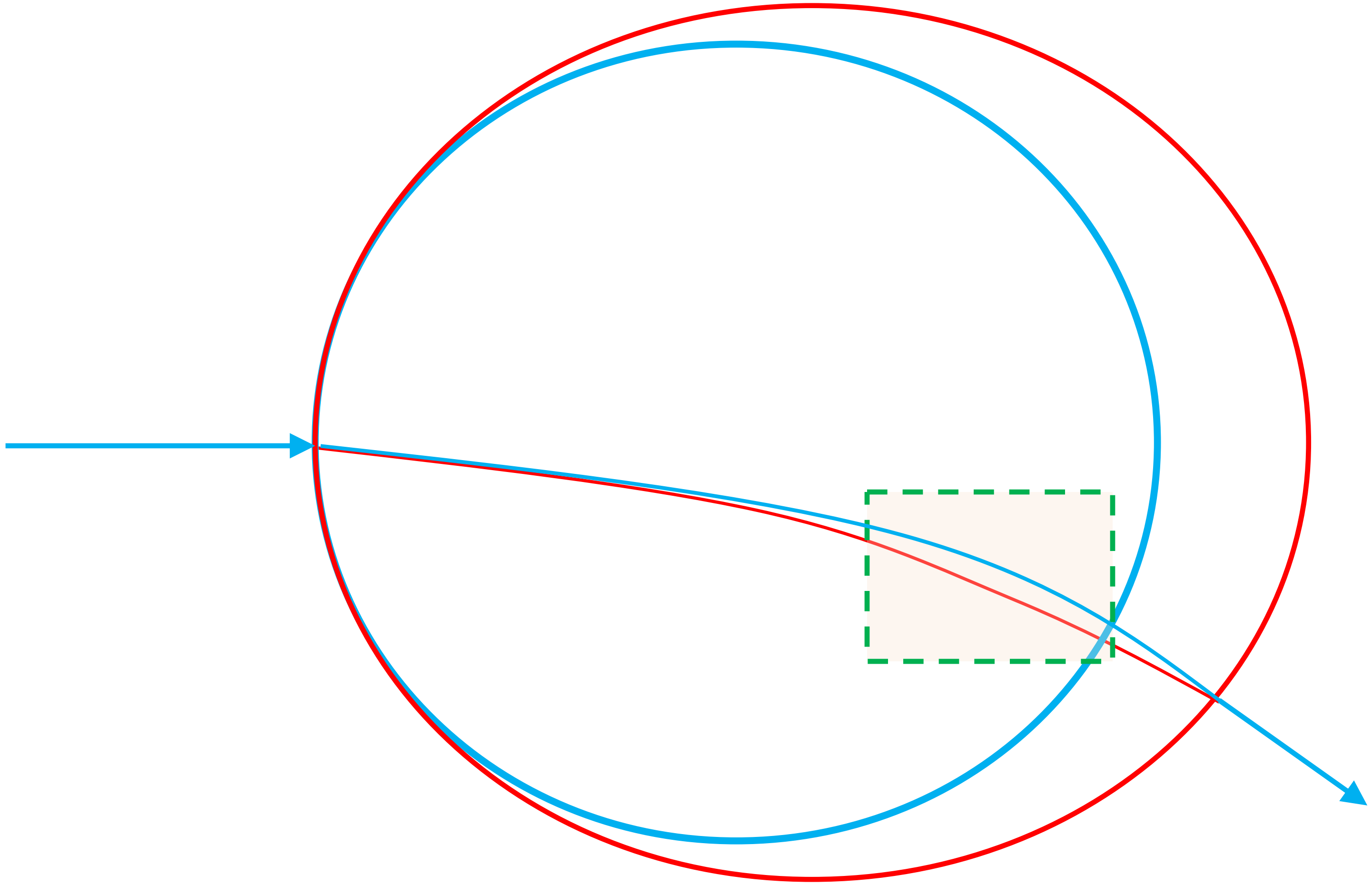

Impact of Object Boundary Inaccuracies

- Can lead to an MLP passing through different voxels

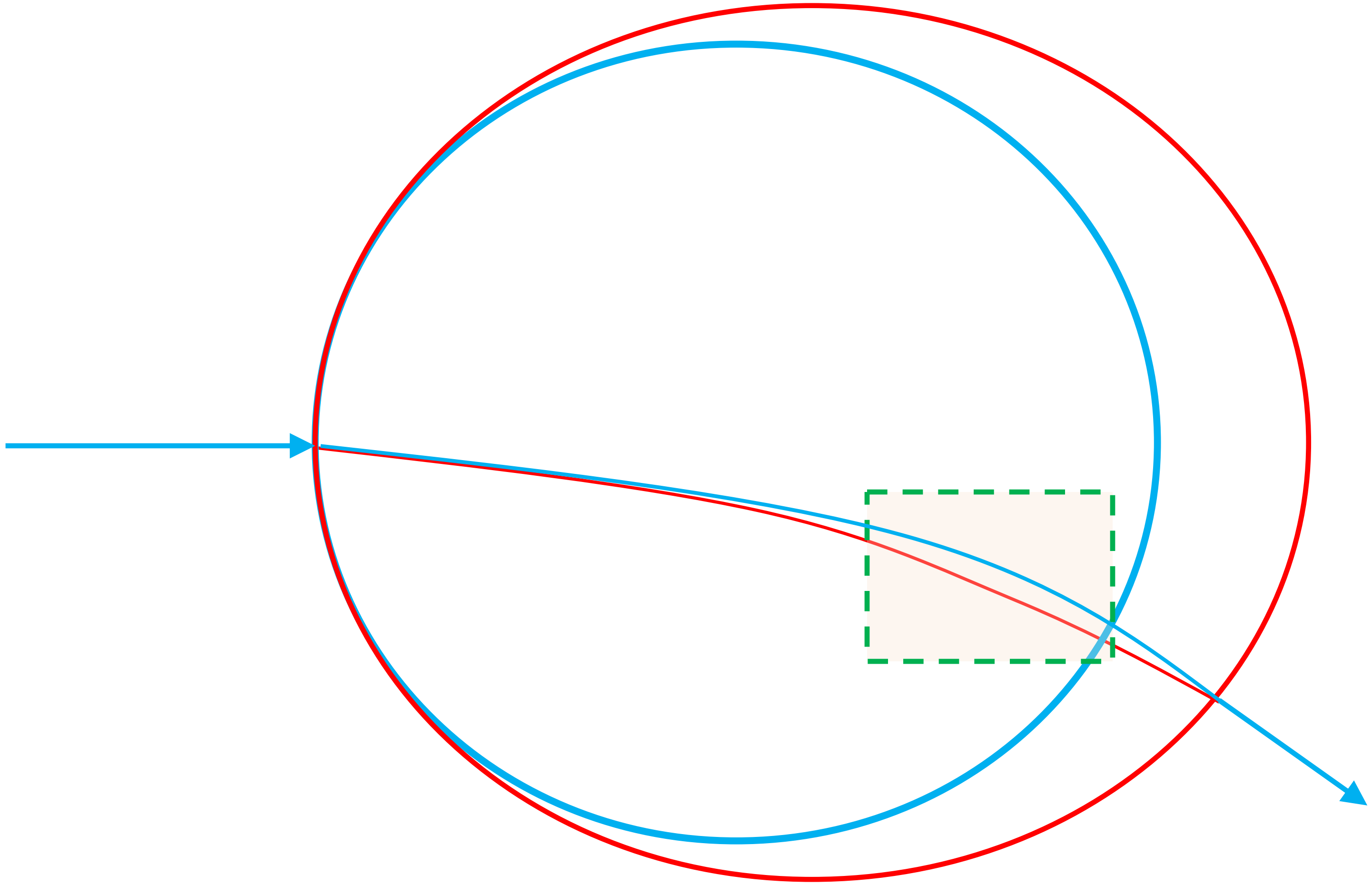

Impact of Entry/Exit Coordinate Inaccuracies

- Can lead to an MLP passing through different voxels (less severe)
- 3D-DDA used to determine exact hull entry/exit coordinates

MLP

where

Equations Before & After Coordinate System Translation + Rotation

$$\vec{y}_{\text{MLP}} = \begin{bmatrix} T_1 \\ \Theta_1 \end{bmatrix} = \left(\mathbf{\Sigma_1^{-1}} + \boldsymbol{R_1^T}\mathbf{\Sigma_2}^{-1}\boldsymbol{R_1}\right)^{-1}\left(\mathbf{\Sigma_1^{-1}}\boldsymbol{R_0}\vec{y}_0 + \boldsymbol{R_1}^T\mathbf{\Sigma_2}^{-1}\vec{y}_2\right)$$

$$\vec{y}_0 = \begin{bmatrix} T_0 \\ \Theta_0 \end{bmatrix} \quad \boldsymbol{R_0} = \begin{bmatrix} 1 & U_1 - U_0 \\ 0 & 1 \end{bmatrix} \quad \mathbf{\Sigma_1} = \begin{bmatrix} \sigma_{T_1} & \sigma_{T_1\Theta_1} \\ \sigma_{T_1\Theta_1} & \sigma_{\Theta_1} \end{bmatrix}$$

$$\vec{y}_2 = \begin{bmatrix} T_2 \\ \Theta_2 \end{bmatrix} \quad \boldsymbol{R_1} = \begin{bmatrix} 1 & U_2 - U_1 \\ 0 & 1 \end{bmatrix} \quad \mathbf{\Sigma_2} = \begin{bmatrix} \sigma_{T_2} & \sigma_{T_2\Theta_2} \\ \sigma_{T_2\Theta_2} & \sigma_{\Theta_2} \end{bmatrix}$$

Coordinate System Translation + Rotation →

$$\vec{y}_0 = \begin{bmatrix} t_0 \\ \theta_0 \end{bmatrix} = \begin{bmatrix} 0 \\ 0 \end{bmatrix}$$

$$\boldsymbol{R}_0\vec{y}_0 = \begin{bmatrix} 0 \\ 0 \end{bmatrix}$$

$$u_2 = \cos\Theta_0\,(U_2 - U_0) - \sin\Theta_0\,(T_2 - T_0)$$

$$\vec{y}_2 = \begin{bmatrix} t_2 \\ \theta_2 \end{bmatrix} = \begin{bmatrix} \sin\Theta_0\,(U_2 - U_0) + \cos\Theta_0\,(T_2 - T_0) \\ \Theta_2 - \Theta_0 \end{bmatrix}$$

Simplified MLP Equations

$$\sigma^2_{t_1}(u_0, u_1) = C(u_1) \int_{u_0}^{u_1} \frac{(u_1 - u)^2}{\beta^2(u) p^2(U)} \frac{du}{X_0}$$

$$= C(u_1) P_1(u_1)$$

$$\sigma^2_{\theta_1}(u_0, u_1) = C(u_1) \int_{u_0}^{u_1} \frac{1}{\beta^2(u) p^2(u)} \frac{du}{X_0}$$

$$= C(u_1) P_2(u_1)$$

$$\sigma^2_{t_1\theta_1}(u_0, u_1) = C(u_1) \int_{u_0}^{u_1} \frac{u_1 - u}{\beta^2(u) p^2(u)} \frac{du}{X_0}$$

$$= C(u_1) P_3(u_1)$$

$$\sigma^2_{t_2}(u_1, u_2) = C(u_2 - u_1) \left[P_1(u_2) - u_2^2 P_3(u_1) + 2u_2 P_4(u_1) - P_5(u_1) \right]$$

$$\sigma^2_{\theta_2}(u_1, u_2) = C(u_2 - u_1) \left[P_2(u_2) - u_2 P_3(u_1) + P_4(u_1) \right]$$

$$\sigma^2_{t_2\theta_2}(u_1, u_2) = C(u_2 - u_1) \left[P_3(u_2) - P_3(u_1) \right]$$

where $C(U) = E_0^2 \left[1 + 0.038 \ln \left(\frac{U}{X_0} \right) \right]^2$

$$\begin{bmatrix} P_1 \\ P_2 \\ P_3 \\ P_4 \\ P_5 \end{bmatrix} = \begin{bmatrix} 0 & 0 & \frac{a_0}{3} & \frac{a_1}{12} & \frac{a_2}{30} & \frac{a_3}{60} & \frac{a_4}{105} & \frac{a_5}{168} \\ 0 & \frac{a_0}{2} & \frac{a_1}{6} & \frac{a_2}{12} & \frac{a_3}{20} & \frac{a_4}{30} & \frac{a_5}{42} & 0 \\ a_0 & \frac{a_1}{2} & \frac{a_2}{3} & \frac{a_3}{4} & \frac{a_4}{5} & \frac{a_5}{6} & 0 & 0 \\ 0 & \frac{a_0}{2} & \frac{a_1}{3} & \frac{a_2}{4} & \frac{a_3}{5} & \frac{a_4}{6} & \frac{a_5}{7} & 0 \\ 0 & 0 & \frac{a_0}{3} & \frac{a_1}{4} & \frac{a_2}{5} & \frac{a_3}{6} & \frac{a_4}{7} & \frac{a_5}{8} \end{bmatrix} \begin{bmatrix} u \\ u^2 \\ u^3 \\ u^4 \\ u^5 \\ u^6 \\ u^7 \\ u^8 \end{bmatrix}$$

MLP Implementation

- Scattering matrices Σ_1& Σ_2 are either:
  - calculated at run time each iteration
  - constructed from lookup table (Σ_1^{-1}& Σ_2^{-1} as well)
- Redundant computations involving fixed (t_2, u_2) precalculated for each MLP

MLP Computational Efficiency

Impact of MLP implementation on single intranode GPU reconstructions:

- ~70% reduction in compute operations
- achieved reconstruction < 10 min clinical feasibility threshold for 1st time
- allows reconstruction times ~6 min on single GPU, ~2 min on 4-GPUs

TVS

Applying Modern Algorithm to pCT

Total variation superiorization is…

- governed by the superiorization methodology (SM) w/ TV as cost function
- a perturbation method for reducing noise w/ minimal edge degradation
- interleaved between FS steps
- preserves convergence of underlying algorithm (e.g. feasibility-seeking) if perturbation resilience is obeyed

- Published: *IEEE Transactions on Medical Imaging* (2020)

An Improved Method of Total Variation Superiorization Applied to Reconstruction in Proton Computed Tomography

BAYLOR UNIVERSITY

TVS Perturbation Calculations & Application Impact

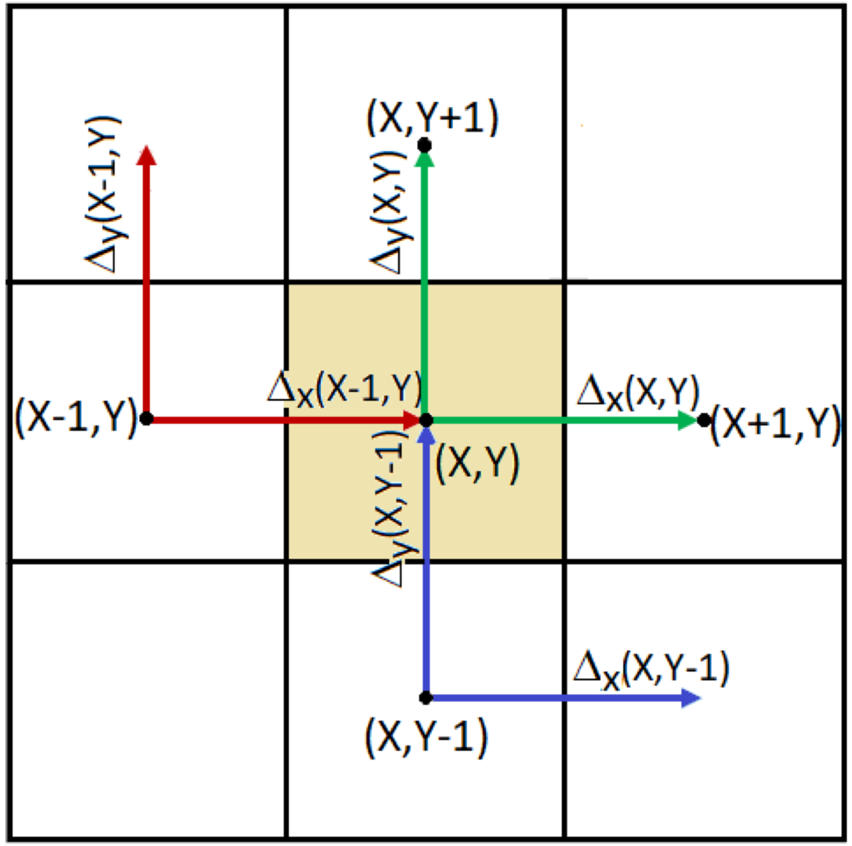

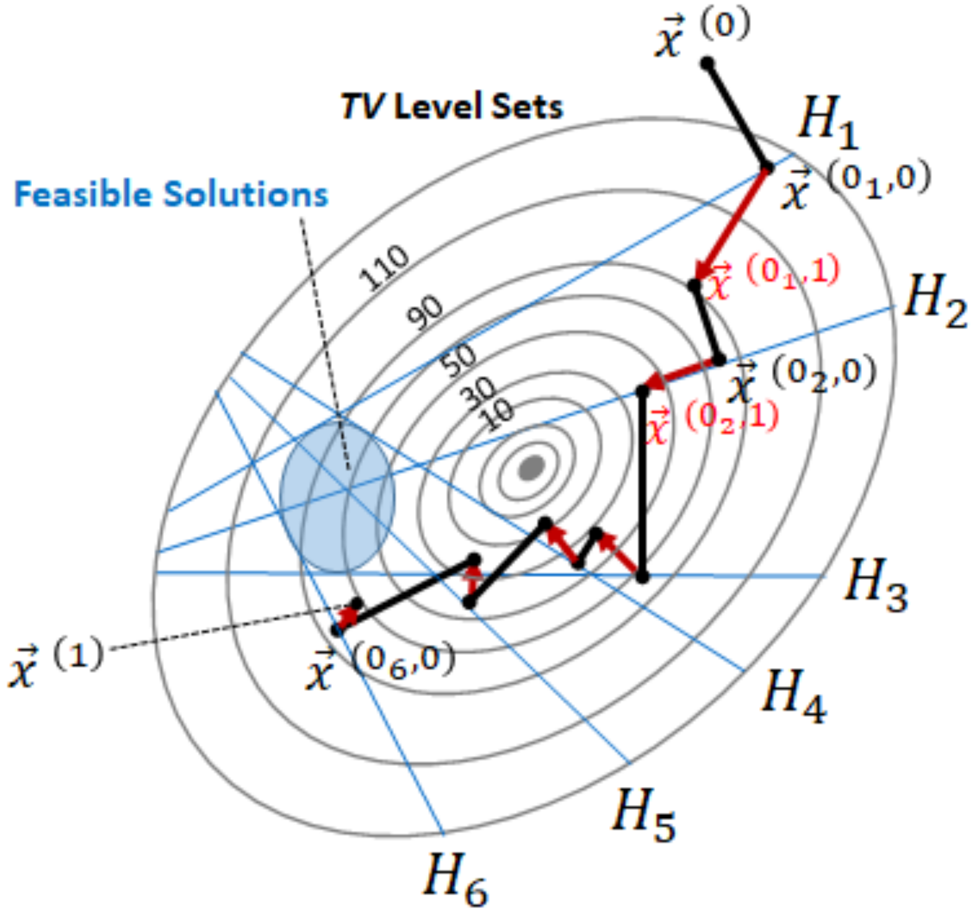

Modernization of TVS Algorithm Used in pCT

- TVS had been shown to benefit pCT imaging but had not been modernized
- Advances in SM led to investigations of the following changes:
  - removal of total variation reduction verification step (TVRVS)
  - added N perturbations per FS iteration
  - perturbation step-size $\beta \leftarrow \beta/2$ replaced by $\beta = \alpha^{\ell}$
    - ($0 < \alpha < 1$ & $\ell \leftarrow \ell + 1$ after each perturbation)
  - added random decrease in $\ell \leftarrow \text{rand}(k, \ell)$ at each FS iteration k

Experimental Results: Analysis of *N*

CTP404 Module

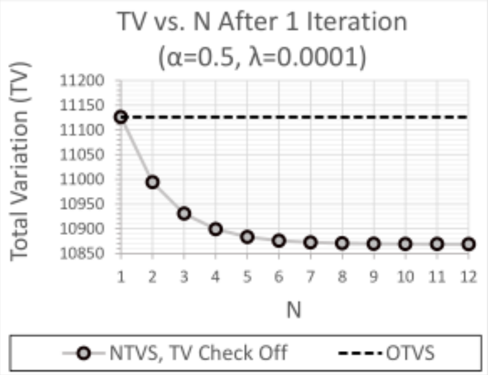

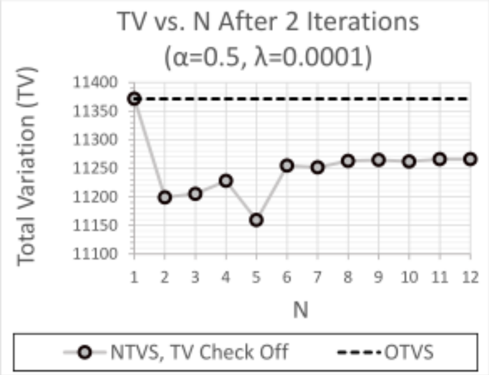

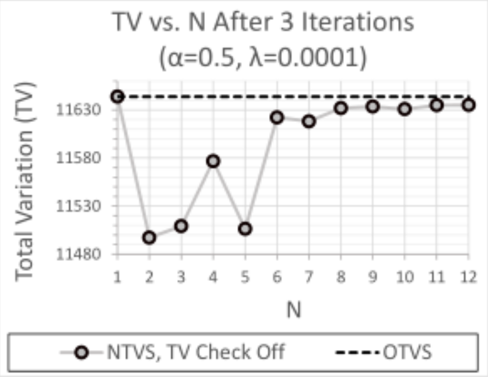

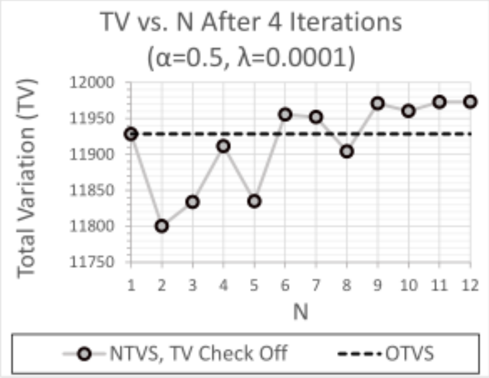

HN715 Head Phantom

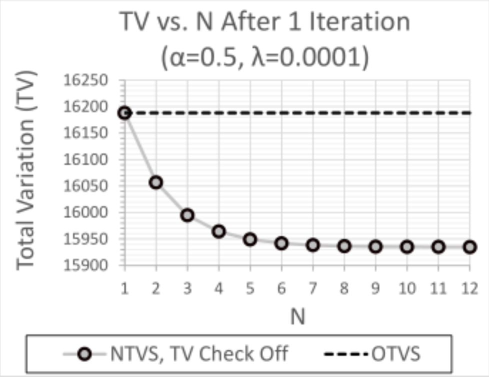

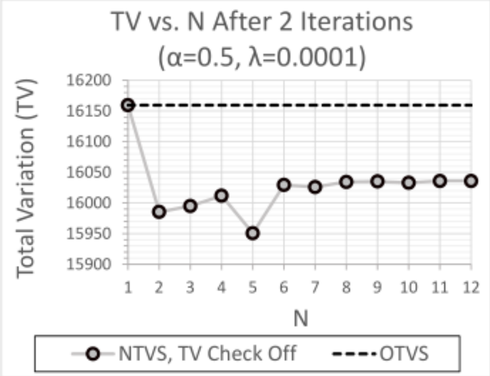

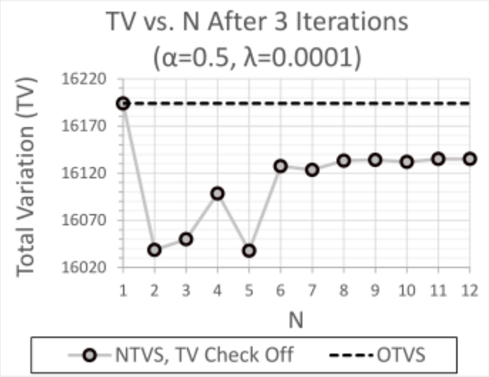

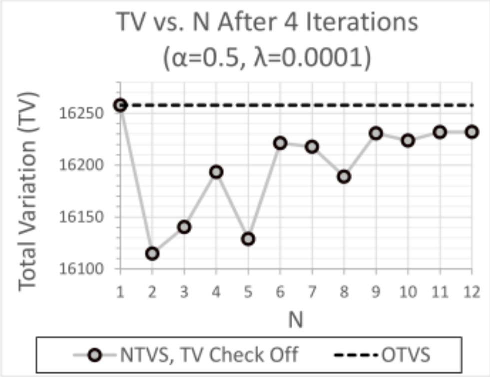

Experimental Results: Analysis of TVRVS ($\alpha = 0.5$)

CTP404 Module

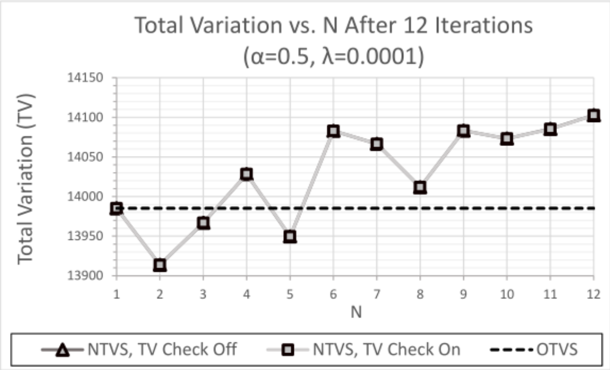

(a)

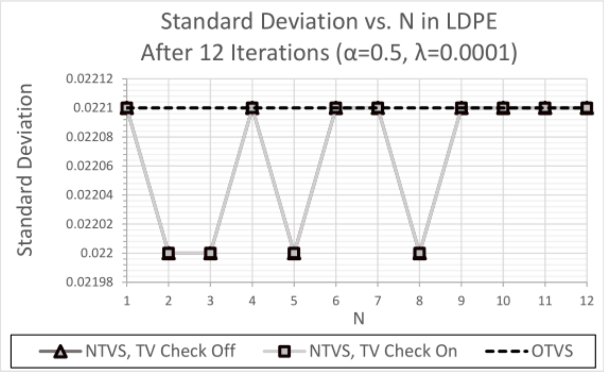

HN715 Head Phantom

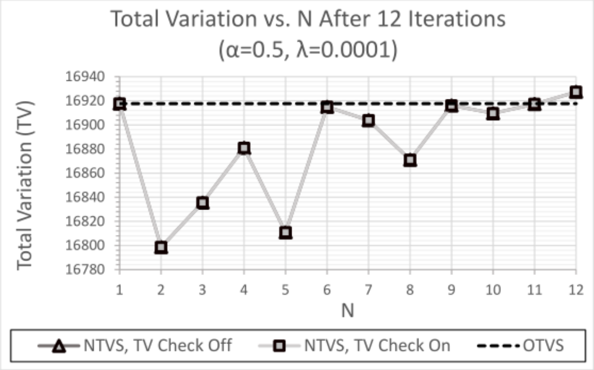

(a)

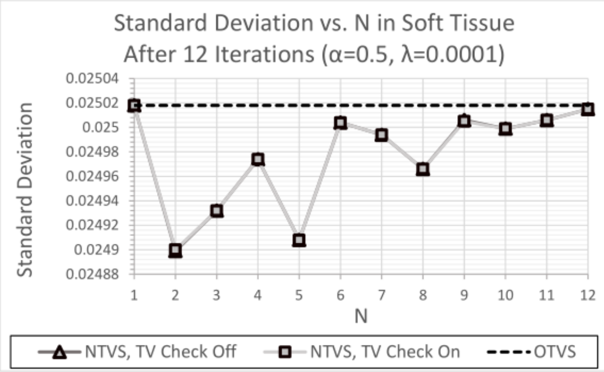

Experimental Results: Analysis of TVRVS ($\alpha = 0.75$)

CTP404 Module

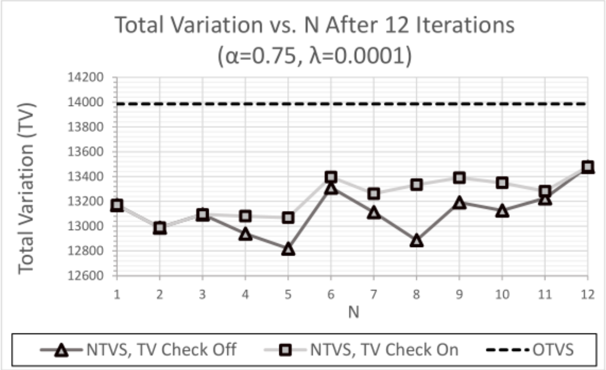

(a)

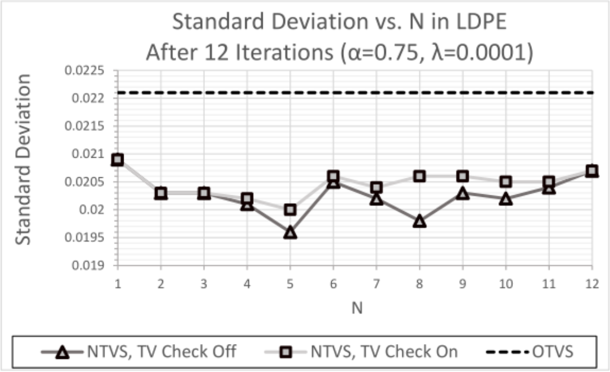

HN715 Head Phantom

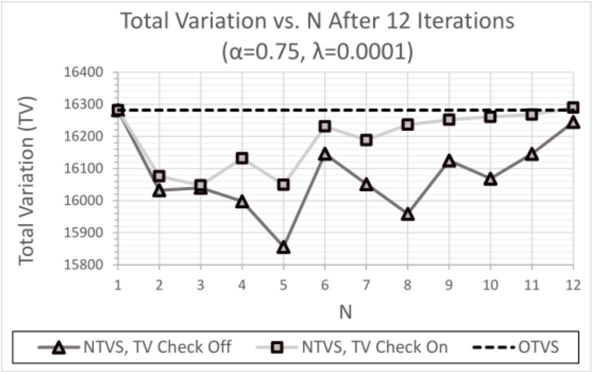

(a)

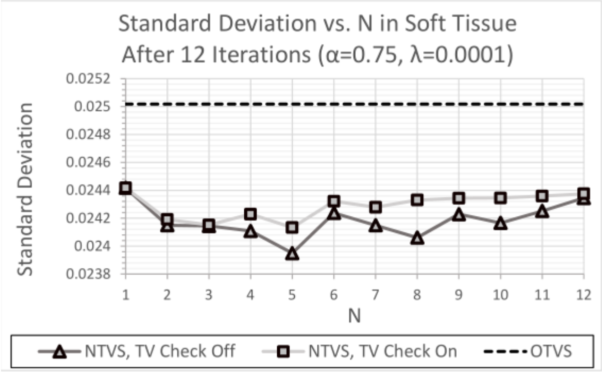

Experimental Results: Analysis of Perturbation Kernel α

CTP404 Module

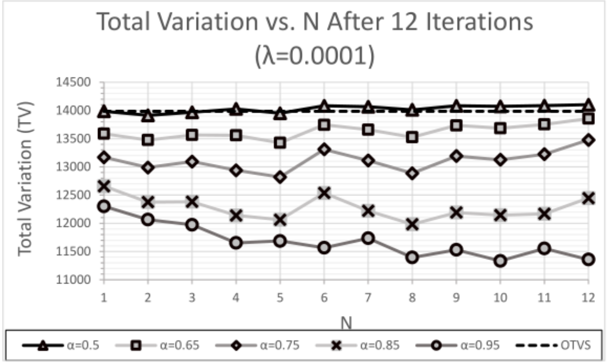

(a)

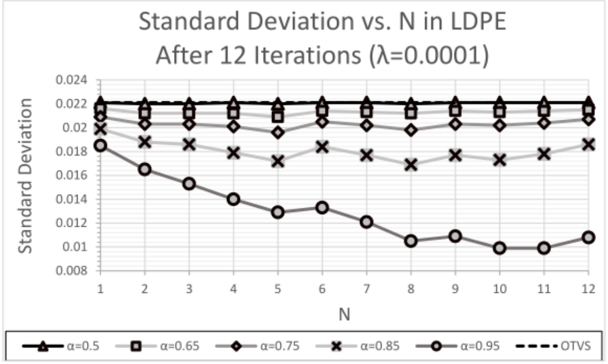

HN715 Head Phantom

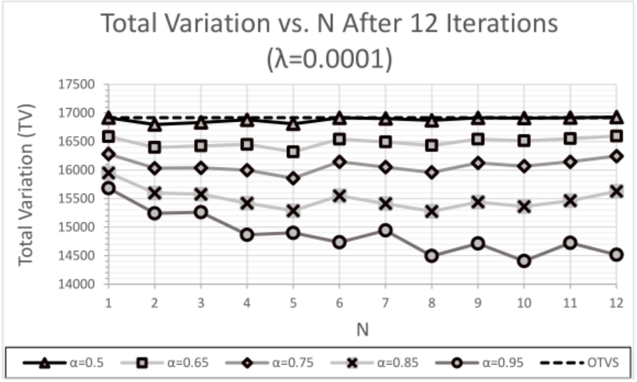

(a)

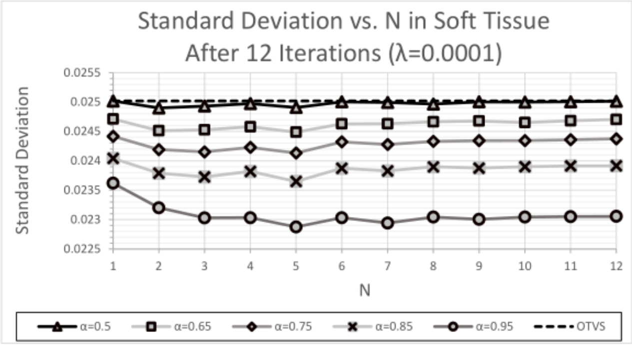

Experimental Results: Analysis of Perturbation Kernel α

CTP404 Module

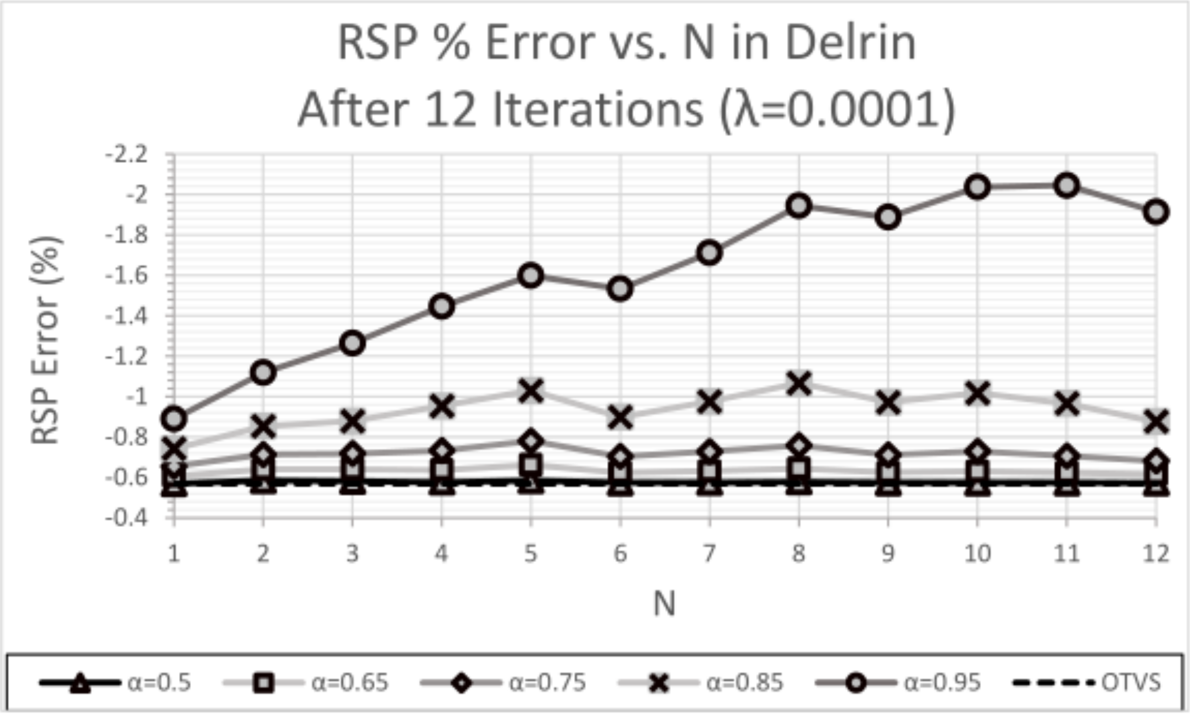

HN715 Head Phantom

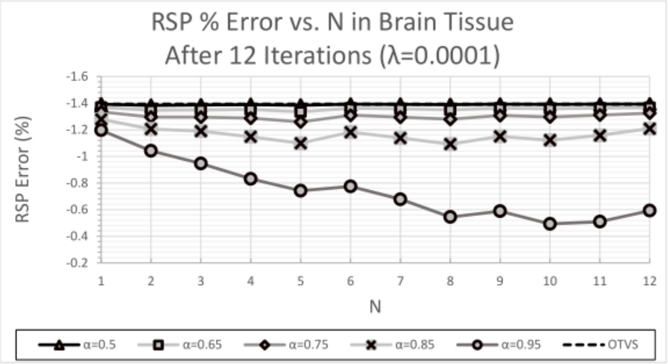

(b)

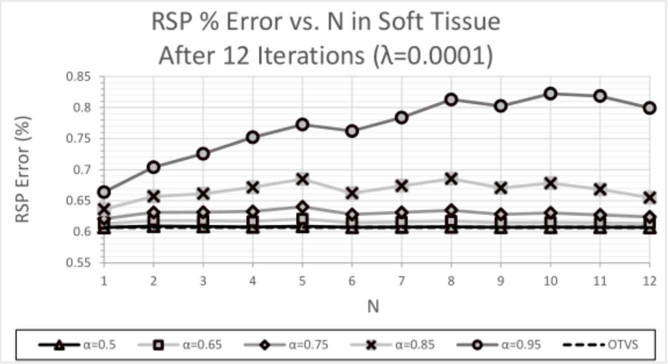

Experimental Results: Analysis of FS Relaxation λ

CTP404 Module

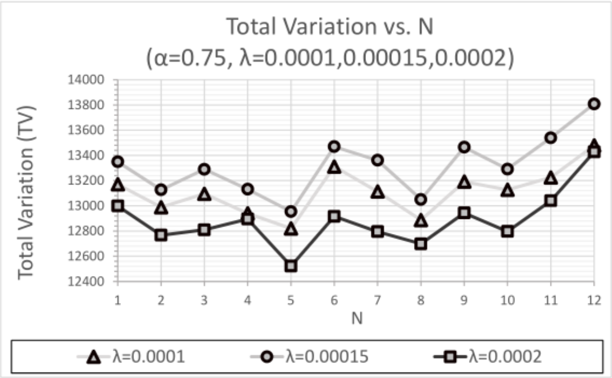

(a)

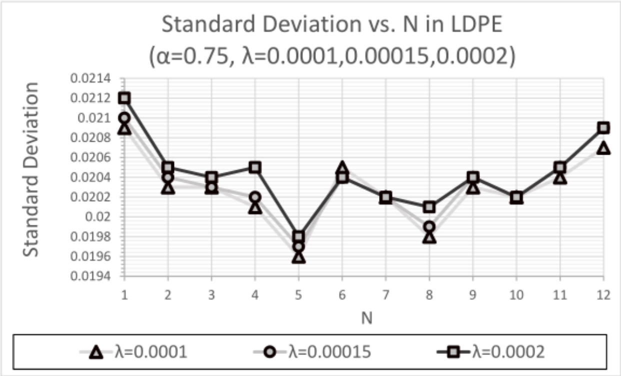

HN715 Head Phantom

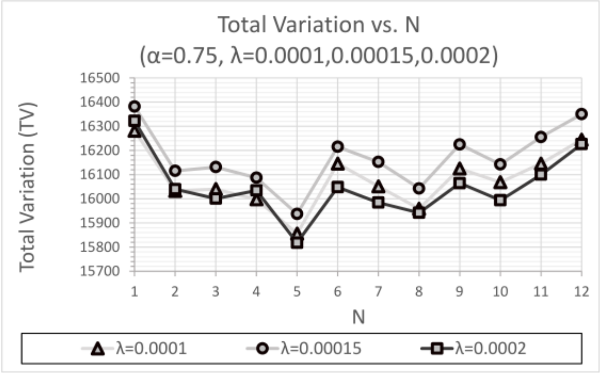

(a)

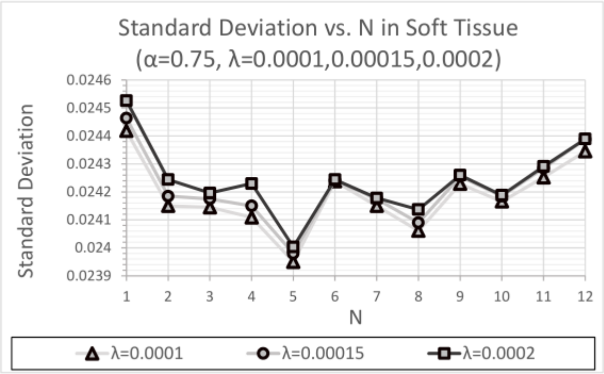

Modern TVS Conclusions

- Removal of TVRVS not harmful, actually often improves TV & σ_{RSP}
- N perturbations per FS iteration beneficial when $3 \leq N \leq 6$, w/ $N = 5$ optimal most often. Performance diminishes for $N \geq 7$, potentially from ℓ increasing too quickly
- $\alpha > 0.5$ offers increasing benefits w.r.t. TV & σ_{RSP}, but $\alpha > \sim 0.75$ increasingly and unpredictably affects RSP convergence, $\Rightarrow \alpha = 0.75$ recommended
- λ can potentially be increased w/o typically observed increase in noise
- future investigations of approaches to uncouple N & β (via ℓ) relationship are needed

Questions or Comments?

Blake_Schultze@baylor.edu

Acknowledgements

- National Institute of Biomedical Imaging and Bioengineering (NIBIB), the National Science Foundation (NSF), award Number R01EB013118, and the United States - Israel Binational Science Foundation (BSF) grant no. 2009012 and no. 2013003.
- The content of this presentation is solely the responsibility of the authors and does not necessarily represent the official views of NIBIB, NIH and NSF.

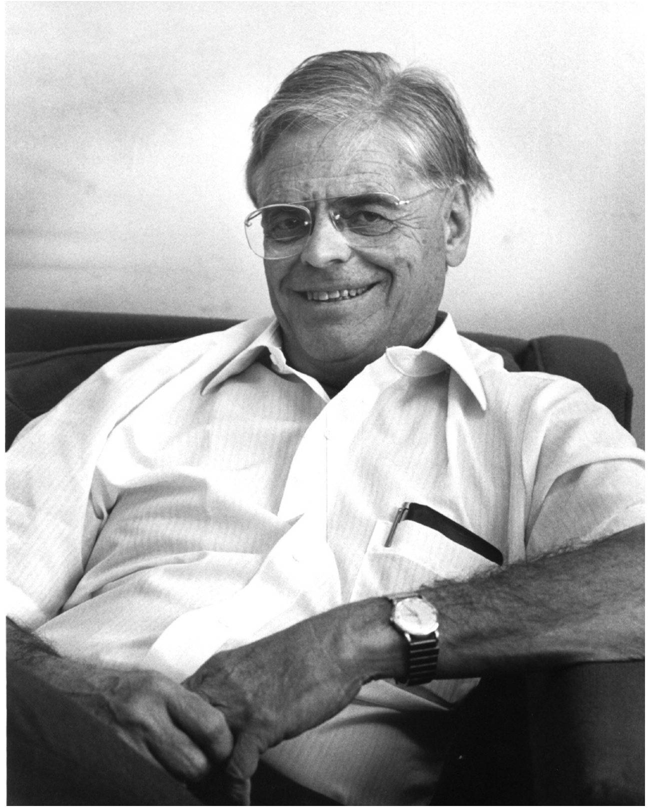

Robert R. Wilson, Ph.D., 1914-2000

Timeline of pCT Work & Publications

2011

Development begins on pCT software w/ intranode GPU parallelization scheme (CSUSB)

2012

Initial Silhouette Carving (SC) hull-detection development begins, published in IEEE NSS-MIC

2013

Development moves to Baylor, now called the BU pCT software

2015

Expanded hull-detection published in Con. Math. Article

Later, achieved <1% RSP error, published in IEEE NSS-MIC

2016-2018

Developed efficient MLP implementation to achieve <10 min image reconstruction times.

2020

Article on modern TVS applied to pCT published in IEEE-TMI

Advantages of Proton Therapy

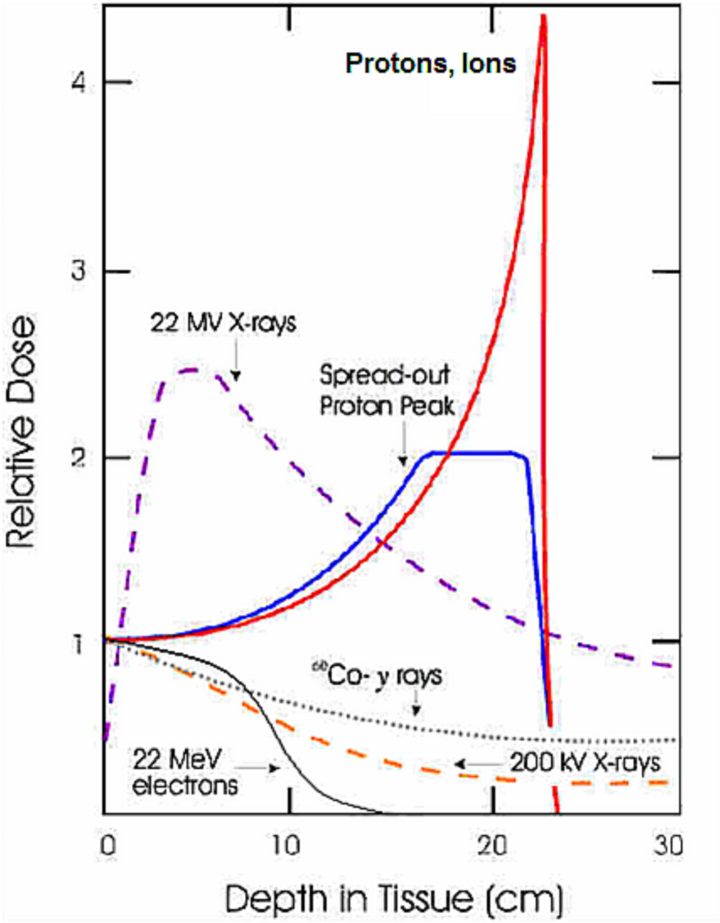

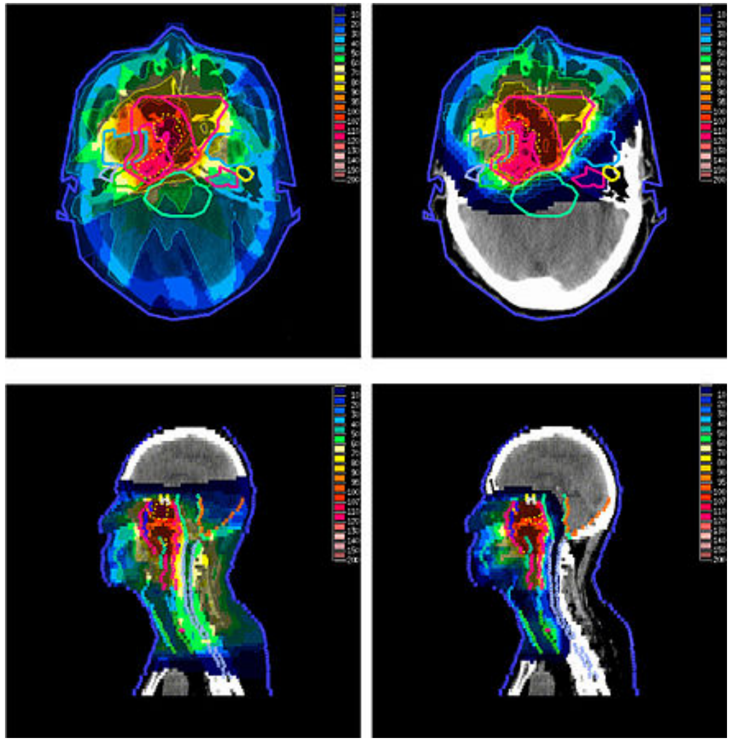

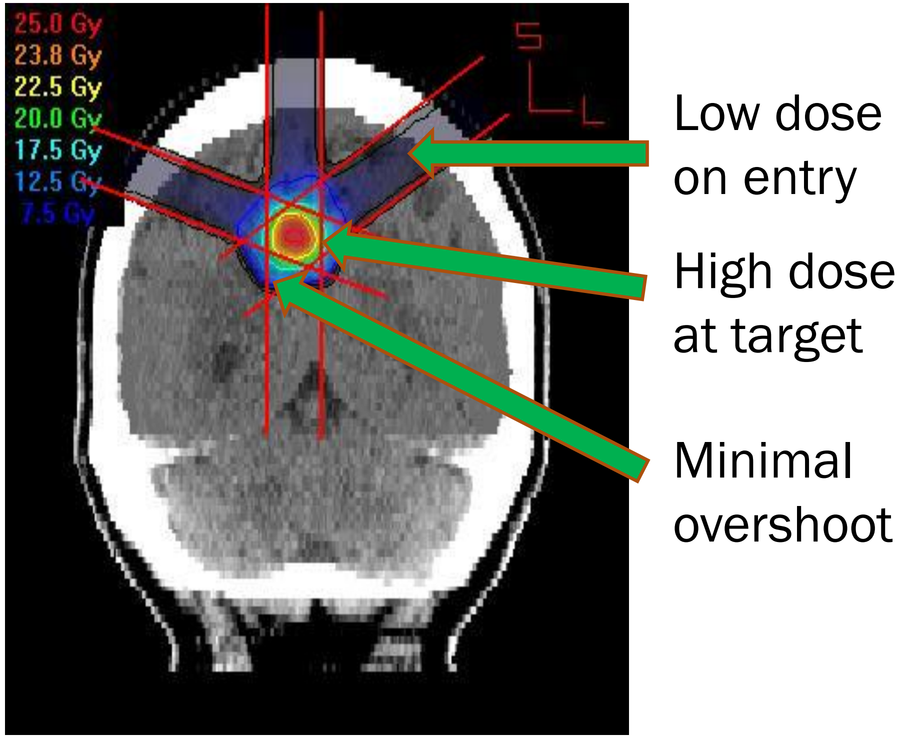

Why pCT for Proton Therapy Treatment Planning

- Conversion of Hounsfield units (HU) to relative stopping power (RSP) adds range uncertainty
- HU-RSP conversion is especially unreliable for some materials
- Common practice 3.5% + 1 mm additional margin to nominal range of proton beam exceeds clinical/planning uncertainty margins of photon therapy
- pCT offers ability to reconstruct RSP directly
- pCT imaging dose much lower than xCT, offering potential for weekly or even daily imaging

pCT Scanner & Data/Image Coordinate Systems

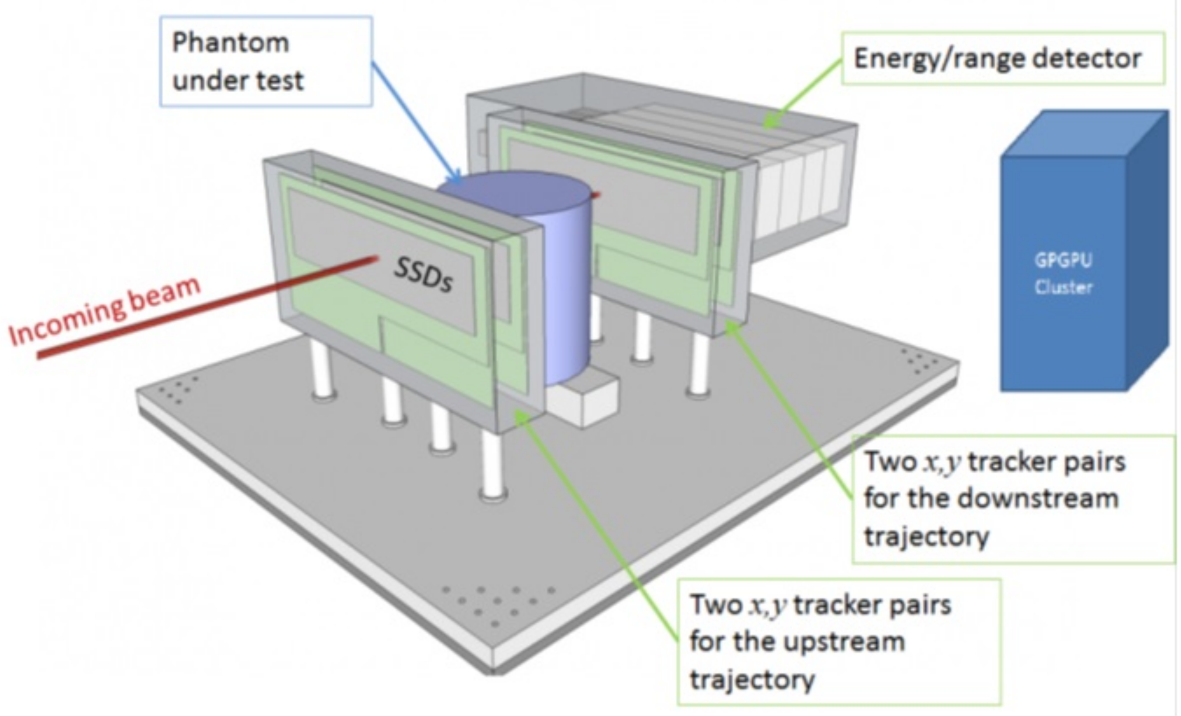

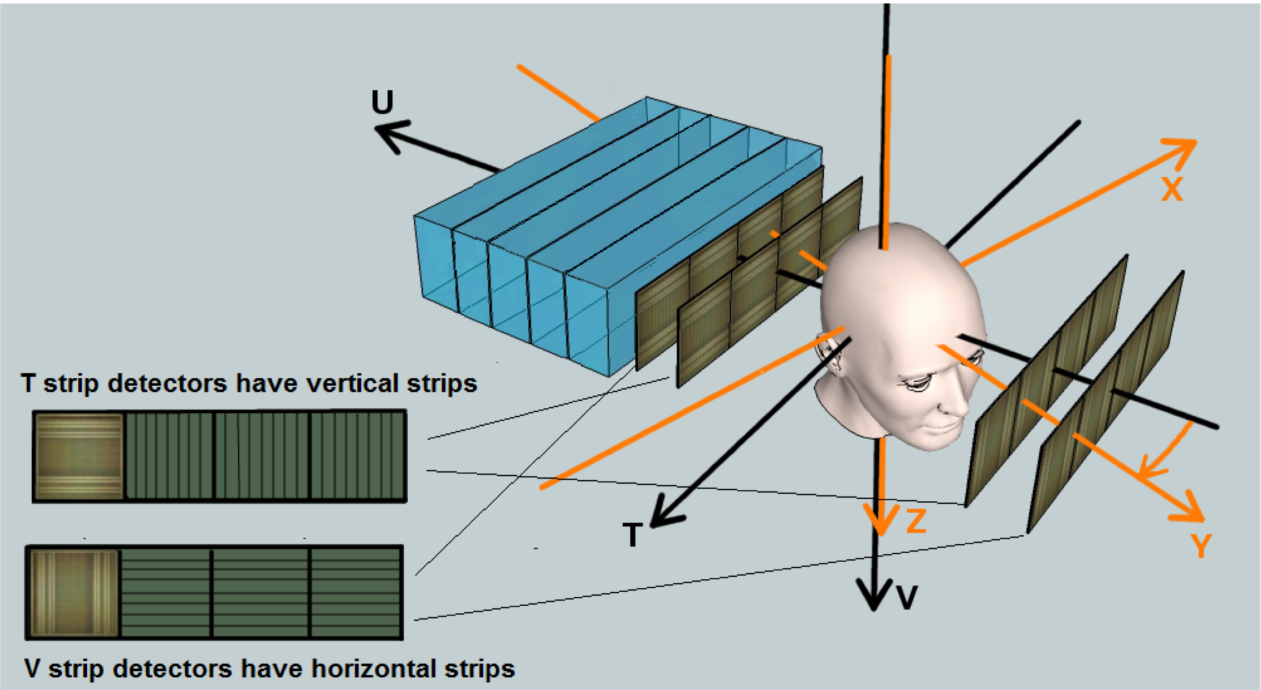

pCT

Fundamentals: Measurement Data & Resulting Linear System

- pCT image reconstruction yields relative stopping power (RSP) map of object
- Energy measurements converted to water-equivalent path length (WEPL) for convenience since

$$\mathrm{WEPL} = \int_{\mathrm{entry}}^{\mathrm{exit}} \mathrm{RSP}(x, y, z)\, d\ell$$

$$\Longrightarrow \mathrm{b_i} = \sum_{\forall j} \mathrm{RSP}_j \cdot a_{ij}$$

- Linear pCT system $\boldsymbol{A}\vec{x} = \vec{b}$ solved using feasibility-seeking (FS) algorithms

BAYLOR UNIVERSITY 1845

Feasibility-Seeking (FS)

Fully Simultaneous (Cimmino type) FS Methods:

Fully Simulataneous DROP Algorithm

- FS performs iterative projections onto rows of $\boldsymbol{A}$, advancing toward feasible (not exact) solution
- Cimmino type FS algorithms project onto all m hyperplanes simultaneously
- Fully Simultaneous DROP (FS-DROP) used herein

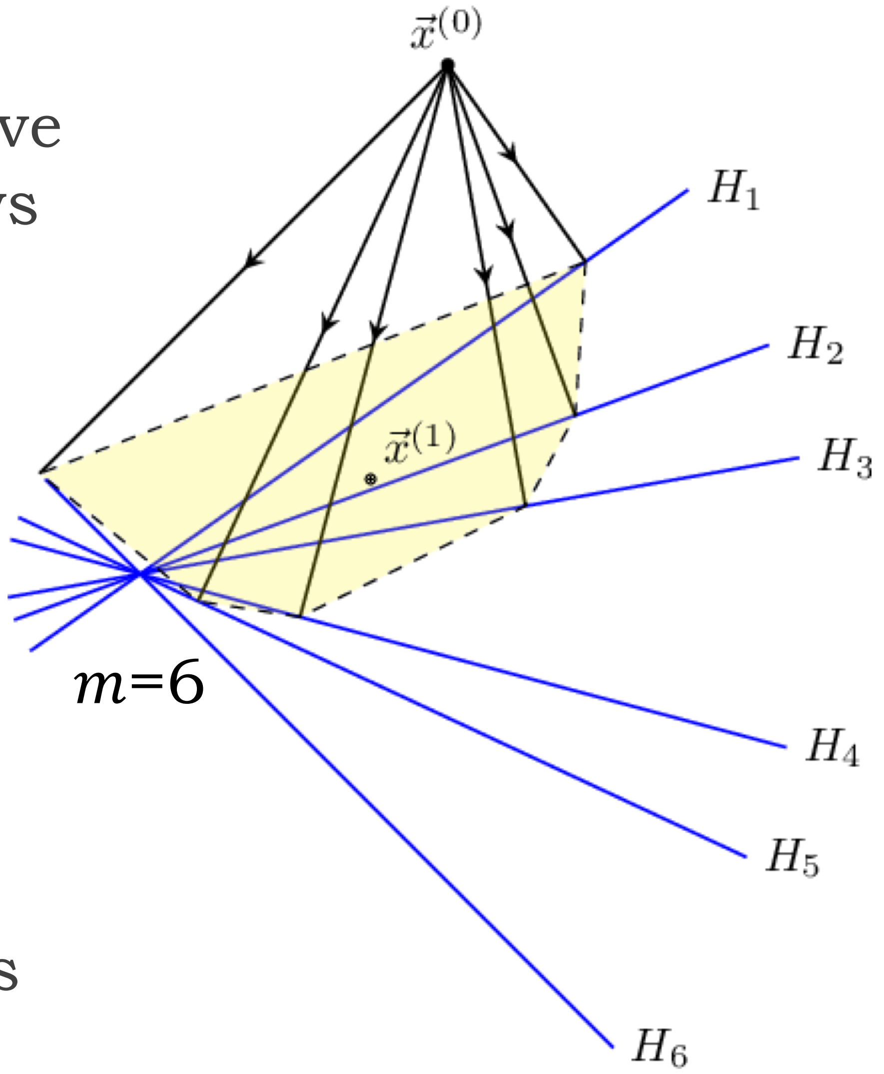

BAYLOR UNIVERSITY

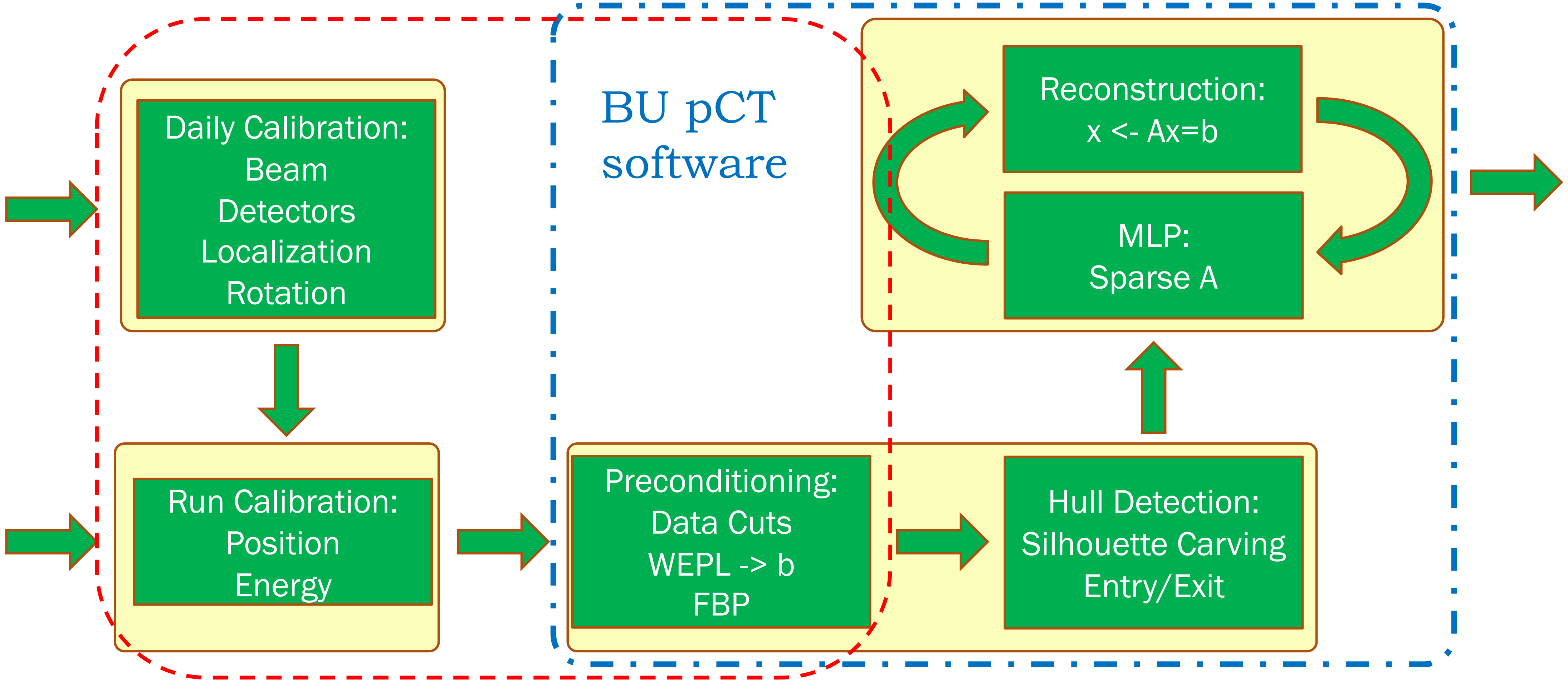

Data Acquisition & Preprocessing

Detailed description published in

Insert	Predicted RSP	Mean RSP	% Discrepancy	Std. Deviation
PMP	0.8770	0.8788	0.1993	0.0201
LDPE	0.9973	0.9990	0.1721	0.0182
Polystyrene	1.0386	1.0390	0.0414	0.0178
Acrylic	1.1550	1.1635	0.7285	0.0199
Delrin	1.3560	1.3532	-0.2059	0.0193
Teflon	1.8280	1.8150	-0.7161	0.0212

RSP Accuracy Achieved

FS-DROP w/ TVS

Original Object Boundary Detection Scheme

Filtered Backprojection Thresholding

Deficiencies of filtered backprojection (FBP) thresholding:

- FBP images noisy & artifact prone due to inappropriate SLP projections
- difficult to select RSP threshold
- produces object interior “holes” where material RSP < threshold
- not useful for excluding voxels outside object
- slow & cannot be performed until FBP complete

BAYLOR UNIVERSITY 1845

Silhouette Carving (SC) Method

- 3D-DDA Development

- 3D-DDA based on 2D ray marching method digital difference analyzer (DDA)
- Fundamentally different than binary decision based steps of 2D algorithms
- Developed numerically stable 3D-DDA, was initially prone to numerical error
- Efficiently & accurately identifies intersected voxels and intersection coordinates